# Transducer Applications Handbook

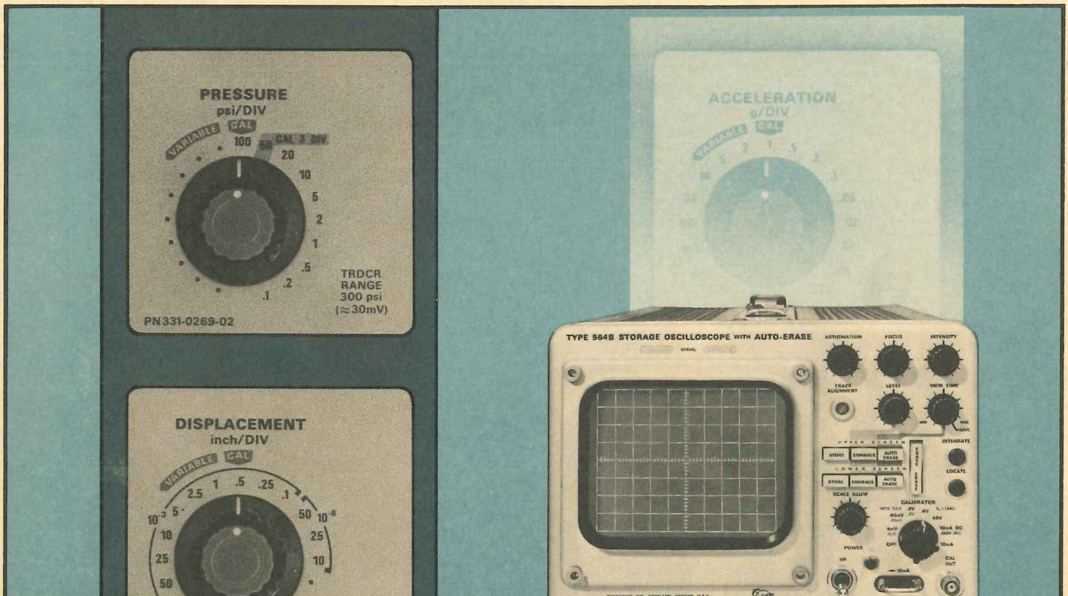


TEKTRONIX®

*committed to technical excellence*

# TRANSDUCER MEASUREMENTS

## Introduction

The oscilloscope has been used as a readout device in transducer measurement systems for many years. Its advantages were not fully realized, however, until Tektronix extended its revolutionary plug-in concept to instruments designed specifically for transducer measurements. With these instruments, a complete transducer measurement system can be housed in a single mainframe. Eliminating the problems created by component incompatabilities, interconnecting cables and overlapping controls.

This handbook contains a brief description of TEKTRONIX Physical Measurement Instrumentation, a few practical application examples, and some reference material useful in making certain transducer measurements. The contents were extracted from "Transducer Measurements," one of the Measurement Concept Series published by Tektronix, Inc. The complete book can be obtained from your local Tektronix Field Engineer, or from Tektronix, Inc., P.O. Box 500, Beaverton, Oregon 97005.

Reprinted in part from Transducer Measurements

- Second Edition 062-1246-02

# 5

# TEKTRONIX TRANSDUCER INSTRUMENTATION

## TYPE 3C66 CARRIER AMPLIFIER

The 3C66 (Fig. 5-1) is a carrier amplifier designed primarily for strain measurement, although it can be used with many other types of passive transducers, including resistive, capacitive and inductive varieties. It can also be calibrated for direct reading of capacitance from 0.2 pF/div to 10,000 pF/div. The unit can be operated in any Tektronix 560-series oscilloscope and requires no external equipment other than the transducer.

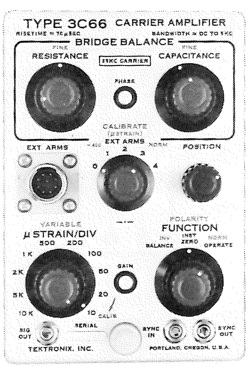


Fig. 5-1.

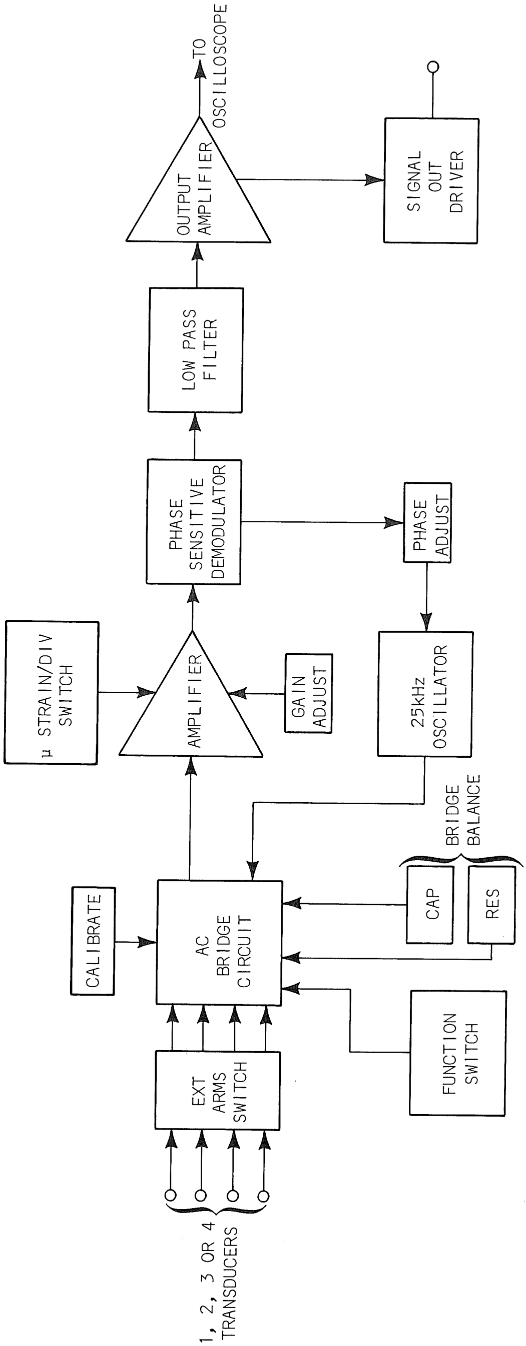


Fig. 5-2. Block diagram, Type 3C66.

block diagram

A block diagram of the 3C66 circuitry is shown in Fig. 5-2. The AC bridge circuit is a conventional 120-ohm Wheatstone bridge, modified to give it additional flexibility. Excitation power at about 5 V RMS is supplied to the bridge by the 25 kHz oscillator, which also provides a reference signal for the phase-sensitive demodulator. Changes in resistance, capacitance or inductance of the transducer or strain gage(s), acting as one or more arms of the bridge, modulate the 25 kHz carrier by unbalancing the bridge. When the bridge is balanced, the carrier is suppressed. The amplifier passes modulation frequencies from DC to 6 kHz, rejecting unwanted frequencies.

In the phase-sensitive demodulator, the 25 kHz carrier is added to the modulated signal so that the output reflects not only the amplitude but the phase of the bridge signal. After passing through a filter circuit to eliminate undesired modulation products, the signal passes to the oscilloscope.

controls

The convenience and flexibility of the 3C66 is revealed by the front panel controls.

The EXT ARMS switch makes it possible to connect from one to four transducers or strain gages as arms of the Wheatstone bridge. (The term "strain gage" will be used in the rest of this discussion to avoid needless repetition. In almost all cases, however, the term "passive transducer" can be substituted whenever it appears.) The 0 EXT ARMS position permits a check of the instrument for normal operation without an external transducer. In position 4 EXT ARMS, the switch connects a standard 4-arm strain-gage transducer directly to the amplifier.

The BRIDGE BALANCE controls adjust shunt capacitance and resistance in the arms of the bridge to offset unbalances caused by the transducer, cable resistance, and capacitance.

The CALIBRATE switch connects a built-in calibrating resistor in parallel to one arm of the bridge, causing a deflection of the trace proportional to the amount of equivalent strain. The GAIN ADJUST control is then manipulated to give the correct vertical deflection of the trace for direct reading in μ strains/div. This adjustment can be used to compensate for different gage factors between strain gages. A provision is also made for changing calibration resistors when the range of the GAIN ADJUST controls is insufficient to achieve the desired deflection. This is only required for other than 120 Ω strain gages.

The μSTRAIN/DIV switch adjusts the sensitivity of the amplifier in ten calibrated steps from 10 to 10,000 με/division of vertical deflection. With active strain gages in all four arms of the bridge, the maximum sensitivity is increased to 2.5 με/div. When the VARIABLE control is activated, the sensitivity may be continuously varied between steps.

The PHASE control permits changes in the phase of the reference signal supplied to the demodulator. The range of adjustment is sufficient to permit use of both resistive, capacitive and inductive transducers.

The FUNCTION switch makes the necessary connections to allow bridge balancing or to completely disconnect the instrument from the system.

The EXT ARMS terminal is a connector to which a shielded four-conductor cable is connected to the strain gages.

gages

The 3C66 can be operated successfully with strain gages ranging from 50 ohms to 2,000 ohms in resistance. Optimum performance and ease of operation are achieved in the 120- to 500-ohm range.

When capacitive transducers are used in conjunction with the internal bridge, the maximum useful sensitivity of the 3C66 is 1.0 pF/div. An external higher impedance bridge increases this sensitivity.

Inductive transducers can be used with good results, although differential transformers designed to operate at 60 Hz are only partially satisfactory at 25 kHz.

Operation of the 3C66 is virtually noise and drift free.

## TYPE Q PLUG-IN UNIT

The Q unit (Fig. 5-3) is designed to be used with Tektronix 530-, 540-, or 550-series oscilloscopes. Its design, operation and capabilities are essentially the same as those of the 3C66.

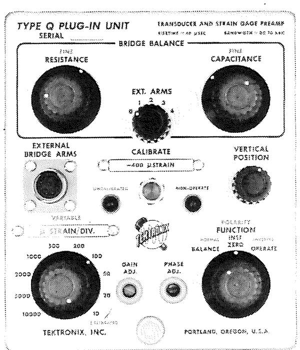


Fig. 5-3.

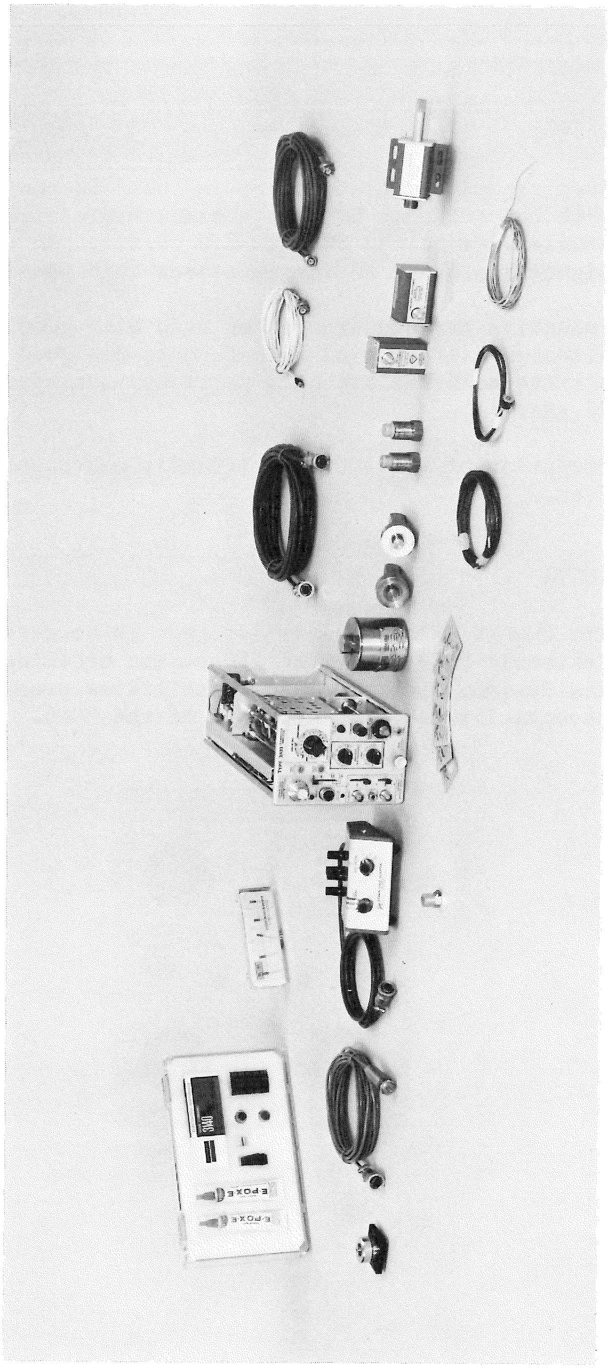

Fig. 5-4. Type 3A10 transducer system.

## TYPE 3A10 TRANSDUCER AMPLIFIER

The Type 3A10 Transducer Amplifier is the most recent addition to the Tektronix line of transducer instrumentation. Together with its family of specially tailored transducers, it constitutes an integrated, all-purpose mechanical measurement system (Fig. 5-4). For the first time, measurement accuracy can be specified for a complete system rather than by individual components. Innovations in system design have eliminated many of the troublesome and time-consuming set-up procedures formerly associated with transducer measurements.

system

At the heart of the system is the 3A10 Transducer Amplifier (Fig. 5-5), a stable, low-noise, wideband DC amplifier of 100% solid-state construction. Both single-ended and differential modes of operation are provided. A 1-11 volt DC power supply (with 60 mA current limit) is included for strain-gage and other voltage-excited transducers. A 10 megohm input impedance may be selected for piezoelectric and other high impedance transducers, while a 1 megohm input permits use of standard oscilloscope probes.

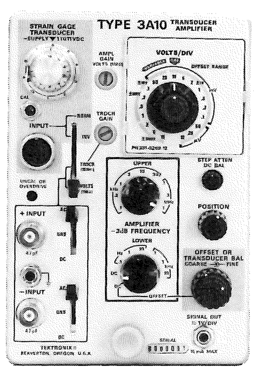


Fig. 5-5.

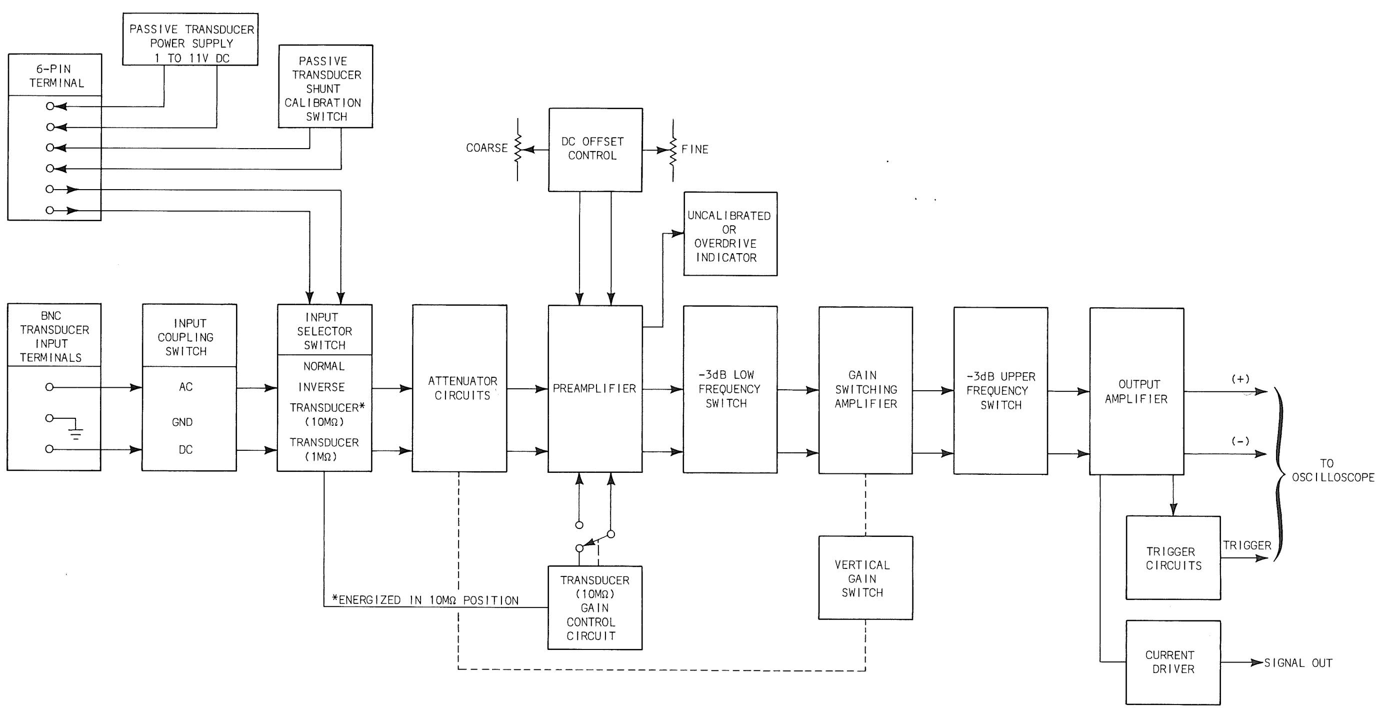


Fig. 5-6. Block diagram, 3A10 transducer amplifier.

transducers

Ten transducers, each tailored specifically for use with the 3A10, and a strain-gage adapter complete the system. With these accessories the measurands of force, relative and absolute displacement, absolute velocity and acceleration, shock, temperature, strain, pressure and many other quantities can be determined. Direct reading in measurand/division is provided by "snap-in" attenuator scales. Each scale is reversible, with appropriate U.S. units on one side and metric units on the other. All strain-gage type transducers are fitted with shunt calibration resistors, eliminating the need for lead-impedance corrections.

A block diagram of the 3A10 circuits is shown in Fig. 5-6. Two BNC terminals are provided for the differential amplifier inputs, and a 6-pin connector for the strain gage adapter and voltage-excited transducers. A Tektronix-manufactured, six-conductor, low-noise cable connects the adapter and transducers to the instrument. Two leads provide the variable bridge excitation voltage, two carry the bridge output signal, and two are used to shunt a calibration resistor in the adapter or transducer to one arm of the bridge. Input coupling switches permit AC or DC coupling, or grounding of either side of the amplifier. Thus, the amplifier can be used in the single-ended mode when desired. An INPUT selector switch controls the polarity of the bridge output signal and the input impedance of the differential amplifier. Ten megohms is presented to the bridge signal and high impedance transducers, while a one megohm impedance is provided for standard oscilloscope probes. In this position of the switch, the instrument can be used as a conventional oscilloscope vertical amplifier.

attenuator

The selected input signal is routed through a calibrated attenuator circuit which is controlled by the gain control switch. This switch also controls the gain of the amplifier. Maximum sensitivity is 10 microvolts/division. No attenuation is imposed on the input signals at sensitivities below 20 millivolts so that a common-mode rejection ratio of 100,000:1 is provided for low-amplitude transducer signals. The gain-control switch is surrounded by a fixture which permits interchanging small metal plates, scaled in appropriate units of pressure, force, velocity, acceleration, etc. Metric units are presented on one side of the plate, while traditional U.S. units are used on the other. This arrangement eliminates "mental scaling" and the attendant possibility of errors in conversion from volts/div to measurand amplitude. A volts/division scale is also provided for conventional oscilloscope measurements. The reverse side of the scale is blank, and can be marked in units of convenience.

pre-amplifier

From the attenuation circuits the signal is applied to a preamplifier where DC offset is controlled. This control acts as the balancing circuit of the amplifier and also functions to "buck out" small DC components of the input signal while maintaining the differential capability. A relay is energized when the INPUT selector switch is placed in the TRDCR position, connecting a variable-gain circuit to the amplifier. This circuit extends the amplifier gain to accommodate differences in transducer sensitivity, and permits switching between inputs without constant recalibration.

bandpass limiting

The lower and upper -3 dB limits of the amplifier bandpass are adjustable, providing selective filtering of signal frequency components. This feature gives a significant flexibility to the amplifier, especially in studies of shock and vibration, where extraneous frequencies often complicate the measurement. The lower -3 dB limit can be varied from DC to 10 kHz, while the upper limit is adjustable from 100 Hz to 1 MHz. Thus, at frequencies below 10 kHz the bandpass can be narrowed to eliminate almost all undesired frequencies, including most externally generated noise. Roll-off is approximately 6 dB per octave. Differentiation takes place on the low frequency slope, while integration may be performed on the upper frequency slope.

gain-switching amplifier

The gain-switching amplifier provides calibrated gain in 1, 2, 5 steps. As stated earlier, no attentuation is imposed on the input signal below the 20 mV/div position. The overall sensitivity range extends from 10 μV/div to 10 V/div.

output amplifier

The output amplifier processes the signal for the oscilloscope mainframe circuits and also provides outputs for the trigger circuit and SIGNAL OUT current driver. The latter circuit provides about 15 mA maximum current drive into 400 ohms, at an approximate 9 V maximum (open circuit). This signal is sufficient to drive many types of recorders without further amplification.

564B/3B4 recommended

The 3A10 amplifier can be used with any of the 560-series oscilloscopes. The 564B with a 3B4 time base is highly recommended, due to the numerous advantages accruing from the split-screen storage capability of the former, and the excellent triggering capability of the time base. The 3A10 can also be stacked in the Type 129 Plug-in Unit Power Supply for multichannel testing and recording, *X-Y* plotting and similar applications.

## SYSTEM ACCESSORIES

Strain Gage Adapter (Fig. 5-7): This device consists primarily of an incomplete 120 Ω Wheatstone bridge, the fourth arm of which is open to accept a strain gage or other passive or active transducer. The EXT ARMS switch permits the use of 1, 2, or 4 external arms. The calibration resistor is placed in shunt with the R4 arm, so that it provides an equivalent of 1,000 μ strains in the 1 and 2 EXT ARMS positions, regardless of the strain gage resistance.

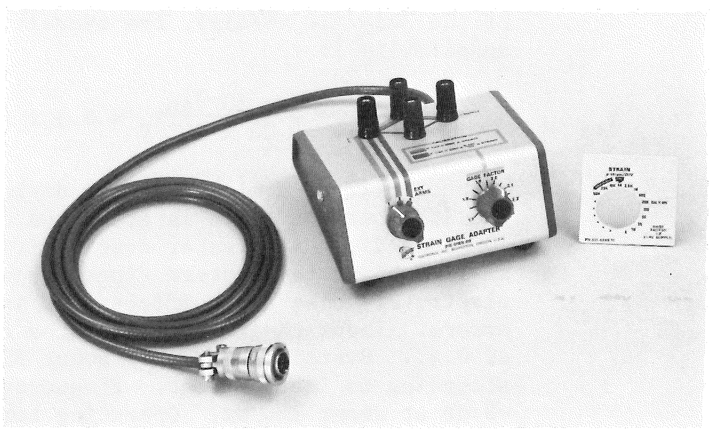


Fig. 5-7. Strain Gage Adapter.

In the 4 EXT ARMS position, of course, the equivalent strain must be calculated. Color coding provides a clear picture of the bridge configuration in all three positions of the switch. The calibration resistor itself is a variable linear precision resistor. This feature eliminates the necessity of calculating equivalent strain when gage factors other than 2 are encountered. GAGE FACTOR range is 1.7 to 2.3. The variable bridge excitation power supply can be adjusted to meet the power density conditions imposed by the particular circumstances of the application (see Appendix). In the 1 EXT ARMS position only 120 Ω strain gages can be used; in the 2 or 4 EXT ARMS positions any value of gage resistance can be used, as long as 60 mA bridge input current is not exceeded. A unique low-noise cable and connector developed and manufactured at Tektronix, connects the adapter to the 3A10.

Displacement Transducer (Fig. 5-8): The displacement transducer consists essentially of an LVDT, an oscillator, a demodulator and a noise filter, all combined in a compact, lightweight package. The DC supply voltage powers an oscillator to provide an AC voltage to the LVDT primary (Fig. 5-9). The output of the secondary winding is applied to the phase-sensitive demodulator, producing a DC output voltage whose amplitude and phase are determined by the position of the core. A simple RC filter suppresses noise in the output signal. The sensitivity of this transducer is approximately 20 $mV/10^{-3}in$. At the highest sensitivity setting of the 3A10 (10 μV/div), the overall system sensitivity is

$$\frac{10^{-5}V}{div} \times \frac{10^{-3}in}{20 \times 10^{-3}V} = 0.5 \times 10^{-6} in/div$$

or about 1/2 of a microinch per division. However, the displacement scale is graduated no lower than 10 μinch/div. At greater sensitivities, even small ambient temperature fluctuations and transducer electrical noise are sufficient to introduce sizable errors. Input range is ±0.2" for a full-throw range of 0.4". System accuracy is about 3% when used according to instructions. Frequency response is -3 dB at about 150 Hz. Operating temperature range is -50° to +60°C (for a typical application, see Chapter 6).

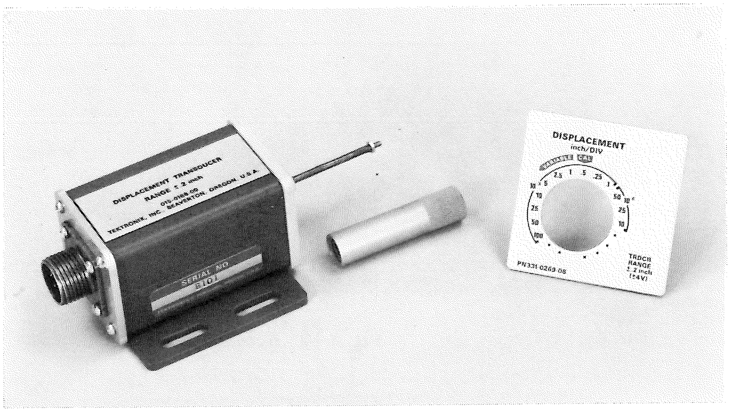


Fig. 5-8. Displacement Transducer.

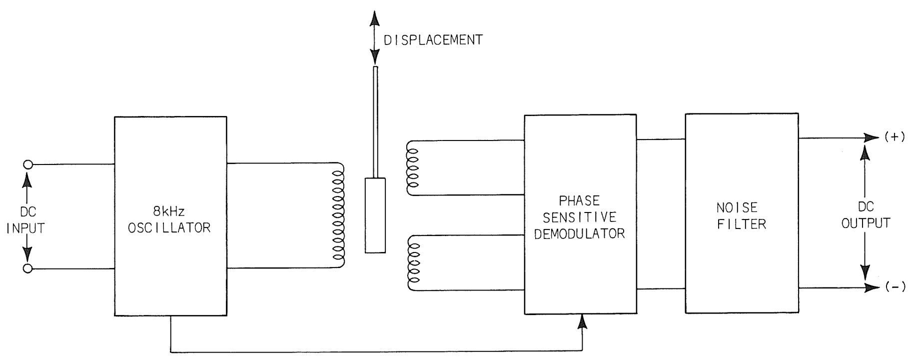


Fig. 5-9. Block diagram, LVDT displacement transducer.

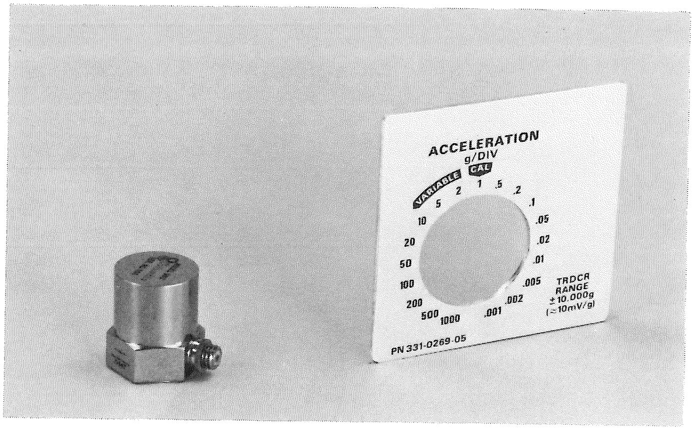


Fig. 5-10. Accelerometer.

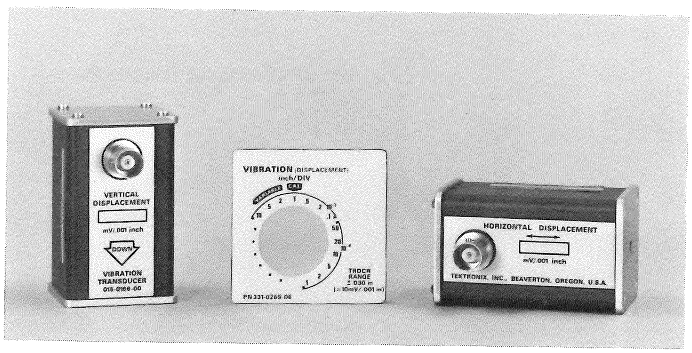


Fig. 5-11. Vibration transducers.

Accelerometer (Fig. 5-10): The accelerometer is a small, rugged, self-generating transducer of the piezoelectric type. The 10,000 pF crystal provides a sizeable output signal when working into the 10 MΩ input impedance of the 3A10. Sensitivity is approximately 10 peak mV/peak g, giving a maximum system sensitivity of about $10^{-3}$ peak g/division. System frequency response (-3 dB) is about 1.5 Hz to 6 kHz. Accuracy is about 5% for the accelerometer and about 8% for the system. Resonant frequency is above 30 kHz. The accelerometer can be used in motion studies to determine absolute acceleration or in shock and vibration studies (see Chapter 6). Special low-noise cable is provided for these applications.

Vibration Transducers (Fig. 5-11): Two vibration transducers, one for vertical and one for horizontal vibration measurements, are provided as system accessories. These devices consist of an inductive (self-generating) seismic mechanical element of very low (8 Hz) natural frequency and a passive integrating circuit (Fig. 5-12). Since the mass is a coil, suspended in the field of a permanent magnet, the coil generates a voltage whenever it is in motion. The amplitude of the voltage is, of course, proportional to the *velocity* of the vibration. This output signal is available at the BNC terminal marked VERTICAL (or HORIZONTAL) VELOCITY (not shown in Fig. 5-11). The same signal is also applied to the passive integrator. Since velocity is the first derivative of displacement with respect to time, the integrated velocity signal is proportional to the absolute displacement of vibration. Shunt resistor $R_S$ provides electrical damping which effectively eliminates the natural-frequency-peak of the device's mechanical-response curve. This provides an almost flat transducer sensitivity down to about 10 Hz. Displacement sensitivity is nominally 10 mV/.001 in, while velocity sensitivity is approximately 600 mV per inch per second. When used with the 3A10 at the highest sensitivity setting of 10 μV/div, therefore, system sensitivity for velocity is 16 x $10^{-6}$ in/s/div and for absolute displacement, $10^{-6}$ in/div. System accuracy is about 8%.

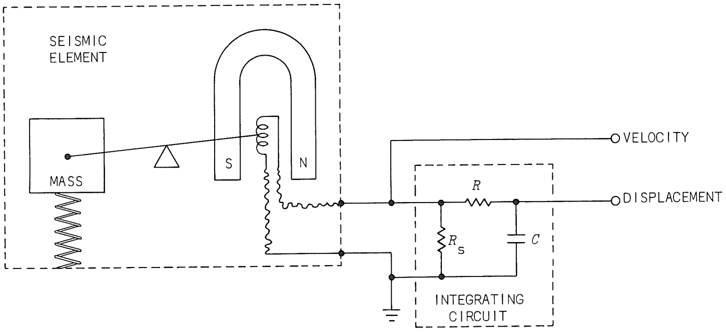


Fig. 5-12. Schematic diagram – vibration transducer.

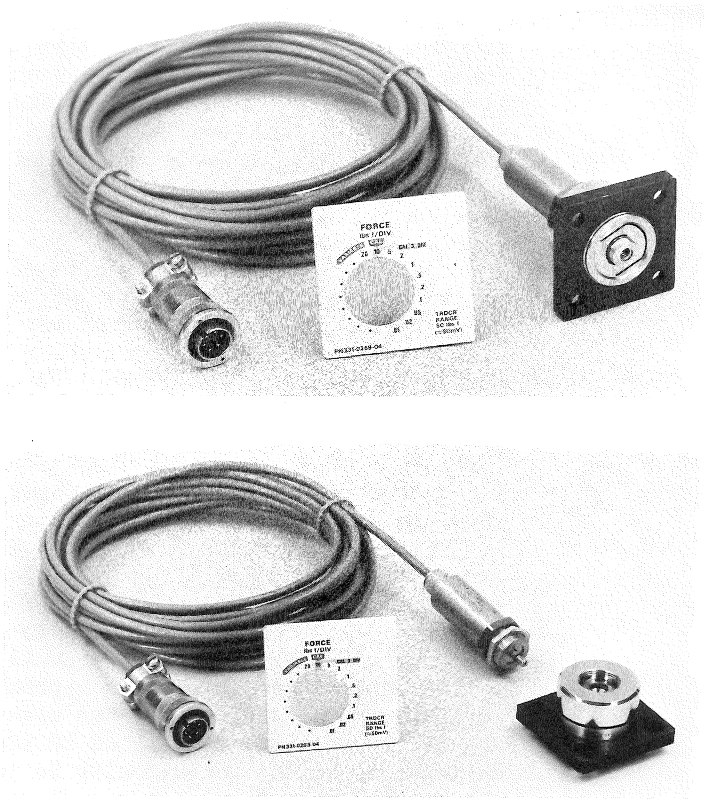


Fig. 5-13. Force transducer (Low).

Force Transducer -- Low Range (Fig. 5-13): The low-range force transducer is actually two transducers in one. It consists of a 50 gram-force universal cell which can be used alone and a 50 pound-force load cell accessory which is attached to the threaded nose of the universal cell.

The sensing element of the universal cell is an unbonded, 4-active-arm strain gage bridge. A selected precision resistor is wired into the connector for convenient shunt calibration of the gram-force/div or pound-force/div scales (Fig. 5-14). This feature considerably increases *system* accuracy, since the calibration is precisely determined for each transducer. Thus, variations in transducer sensitivity are automatically compensated for, eliminating a common source of readout error.

Maximum useful system sensitivity is 0.01 gram/div with a system accuracy of about 5%. Small displacements can also be measured with this device. Maximum displacement range is .12 mm.

The load cell accessory increases the force range to 50 pound-force. Deflection of the load cell accessory diaphragm under tension or compression is communicated to the universal cell through an adjustment screw. This screw is used to bias the load cell for tension or compression measurements. Maximum system sensitivity of the 50 pound-force configuration is 0.01 pound-force/div or 5 gram-force/div with an accuracy of approximately 5%.

Force Transducer -- High Range (Fig. 5-15): The high-range force transducer is a simple 3,000 pound-force load cell, consisting of a steel cylinder to which a strain gage bridge has been cemented, all contained in a hermetically sealed housing. Both ends of the cylinder are threaded to accept heavy duty eyebolts, or a "load button" for compressional loads.

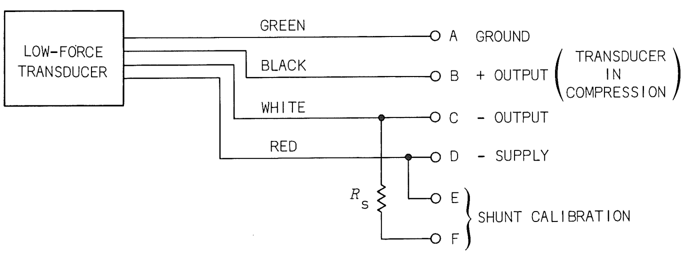


Fig. 5-14. Shunt calibration resistor installation.

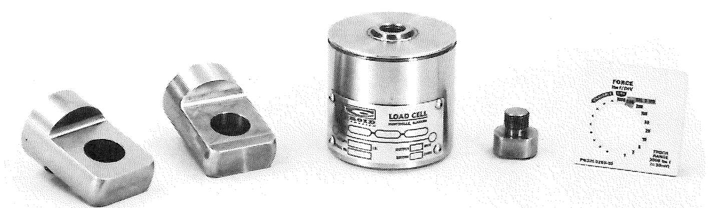


Fig. 5-15. Force transducer (High).

A manufacturer-installed half-full-scale shunt calibration resistor is also included. Bridge excitation power, bridge output signal and shunt calibration resistor leads are wired to a Bendix connector for easy hook-up to the 3A10. Maximum useful system sensitivity is 1 pound-force/div or 0.5 kilogram-force/div, with a system accuracy of about 4%.

Pressure Transducers (Fig. 5-16): Two pressure transducers of identical design but different pressure ranges are available as accessories to the 3A10. The 3,000 PSI transducer is intended primarily for hydraulic pressure measurements and high pressure compressors. The 300 PSI model will be more often used in air- or gas-pressure measurement. Construction is very simple. A strain gage bridge, bonded to a diaphragm, senses any distortion of the diaphragm due to fluid pressure. A factory-installed calibration resistor is built into the bridge. Bridge and shunt calibration leads are wired to a 6-pin connector. The pressure inlet is designed to meet Mil Spec 33649-4 (1/4" tubing, fluid connection, female) formerly Air Force Navy 10050-4, which requires internal straight thread 7/16" 20 VNJF-3B. The positive O-ring sealing action and ease of connection provided by this design can be attained with a wide variety of reducers, adapters and similar fittings. Maximum useful sensitivity of the system is 1 PSI/div with the 3,000 PSI sensor and 0.1 PSI/div with the 300 PSI sensor. System accuracy is about 4% with either transducer.

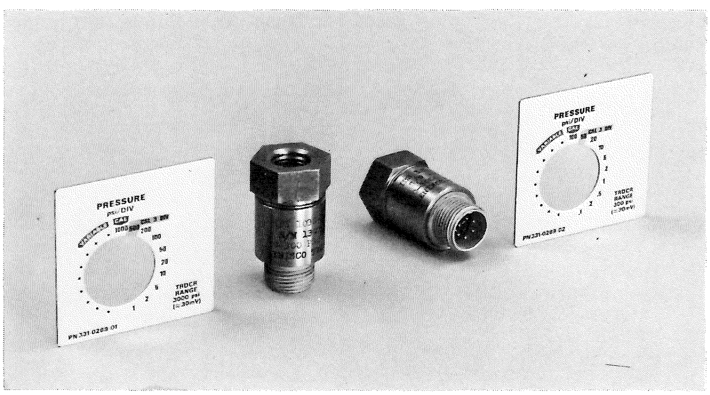


Fig. 5-16. Pressure transducers.

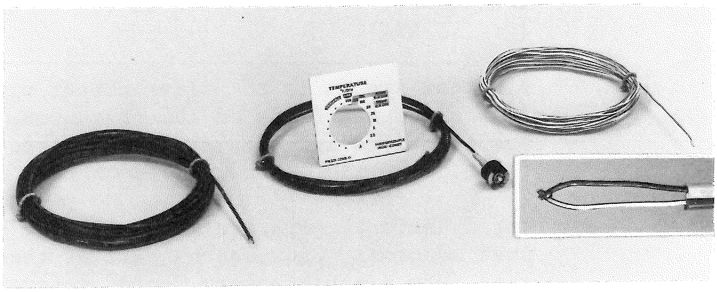

Fig. 5-17. Thermocouples.

Temperature Transducers (Fig. 5-17): Three thermocouple-type temperature sensors are available as accessories to the 3A10 system. Two of these devices consist of lengths of #30 iron-constantan thermocouple wire, one end of which has been spot-welded to form a thermoelectric junction. One 20-foot length is insulated with silicone-impregnated glass braid, giving it a maximum temperature range of 900°F. Another 20-foot length is insulated in color-coded polyvinyl, extruded onto the bare wires and bonded in rip-cord construction without further insulation. This insulation will stand up to 220°F and shows excellent resistance to abrasion, petroleum, alkalies, etc. The third thermocouple is made from #24 wire, insulated in impregnated glass braid. It is six feet long and fitted with a magnetic coupling device at the junction end. This device holds the junction in firm contact with ferrous materials while temperature measurements are made.

Each of the thermocouples generates about 30 μV/°F from 50°F to 900°F. Maximum useful system sensitivity is thus 0.5°F/div, with an accuracy of about 5%.

If a stable reference junction is required, a second thermocouple may be connected in series with the active one, and immersed in a temperature-controlled, nonconductive liquid, such as oil or distilled water (Fig. 5-18A).

A better system is to solder copper wires to the iron and constantan leads of the thermocouple and immerse the junctions in a fluid, as described above. (Fig. 5-18B).

For dynamic temperature measurements, the binding post adapters (provided as part of the thermocouple kit) form a satisfactory "cold" reference junction in almost all cases.

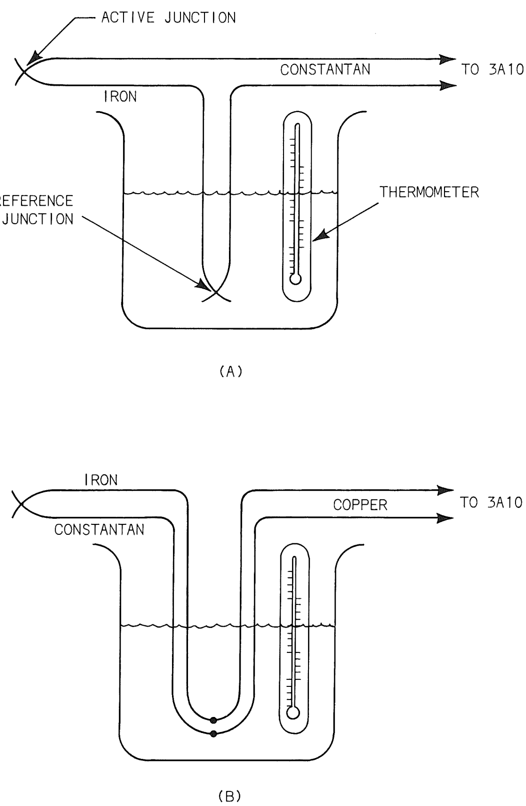


Fig. 5-18. Establishing thermocouple reference junctions

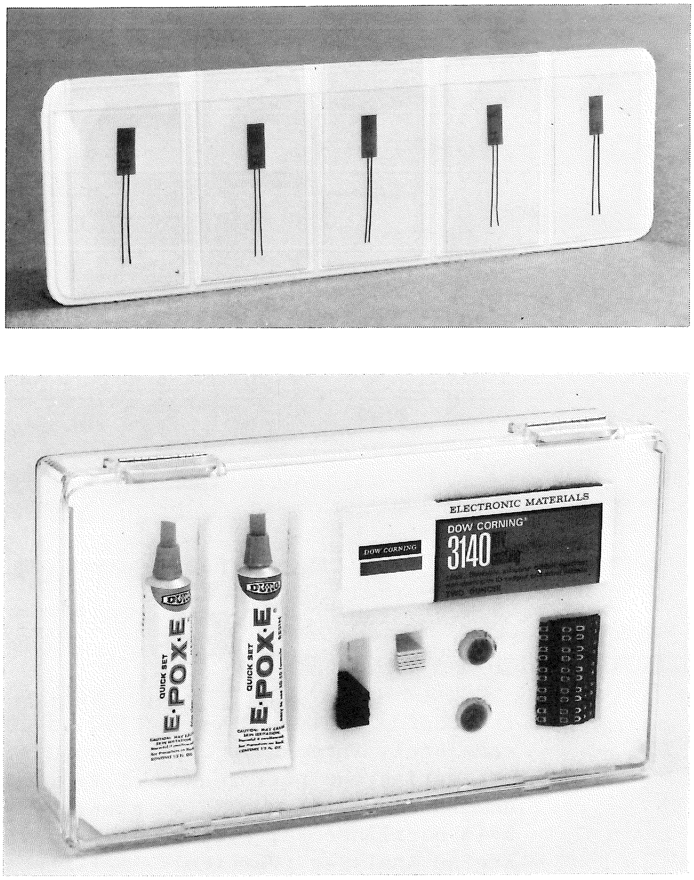


Fig. 5-19. Strain gages and strain gage kit.

Strain Gages and Strain Gage Kit (Fig. 5-19): A package of five strain gages and a complete strain-gage application kit complete the 3A10 system accessory list. The strain gages are 120 ohm, metal-foil, polyimide-backing precision gages with a nominal gage factor of 2 and a gage length of 1/8". When used with the Strain Gage Adapter at 4 volts DC, the strain-gage maximum system sensitivity is 5 μstrains/div with an accuracy of about 3%. Maximum range exceeds the yield point of common metals.

The strain gage kit contains the basic materials required for cementing and waterproofing the gage and connecting the cable to the strain gages.

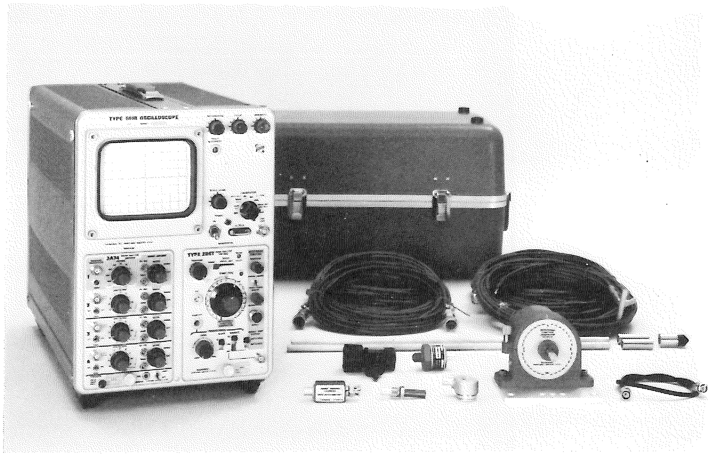

Fig. 5-20. Engine analyzer system.

## TEKTRONIX ENGINE ANALYZER SYSTEM

The Engine Analyzer System (Fig. 5-20) is a completely integrated oscilloscope system for evaluating the performance of reciprocating engines, compressors and pumps. It consists of a 561B or 564B oscilloscope, fitted with a modified 3A74 Engine Analyzer (Vertical) Amplifier and a modified 2B67 Engine Analyzer (Horizontal) Time Base, a Rotational Function Generator (RFG) and four transducers, plus the necessary connecting cables. The transducers sense cylinder pressure, ignition voltage, vibration and cylinder top dead center (TDC). The first three quantities are displayed against crankshaft angle, a function generated in the RFG and reference to TDC. A modified sinewave, representing cylinder volume, is also generated in this device. Many malfunctions such as incorrect timing, faulty ignition, valve leakage, piston slap and others can be diagnosed, by interpreting the display. Costly routine overhauls can thus be avoided and down time kept to a minimum. At the same time, serious malfunctions can be detected and corrected before damage occurs.

A complete description of the Engine Analyzer System and its components, together with helpful information on applications, may be found in the Tektronix Measurement Concepts book, *Engine Analysis Measurements*.

## TYPE 410 PHYSIOLOGICAL MONITOR

The Type 410 is a highly specialized medical transducer system, designed primarily as a patient monitor (Fig. 5-21). It consists of an oscilloscope-type display device and a number of electrical pickups for making ECG, EEG, pulse and other physiological measurements. It can be operated from AC line voltages or its own internal battery pack. It is used extensively in the operating room, intensive care unit and during patient recovery.

The Type 410 is described in the Tektronix Measurement Concepts book, *Biophysical Measurements*.


Fig. 5-21. Type 410 Physiological Monitor.

# 6

## PRACTICAL APPLICATIONS

The range of measurements which can be performed with transducer systems is limited only by the imagination and ingenuity of the user. A few examples of practical applications are presented in this chapter to illustrate the basic principles involved. The applications selected for each transducer are generally typical of those encountered in industry. All measurements were performed with the 3A10 Transducer System, using a Type 564B (Storage) Oscilloscope and a C-12 camera.

### MISCELLANEOUS APPLICATION NOTES

**bonded resistance strain gage**

Bonded resistance strain gages are the most widely used of all types of transducers. This is due primarily to their versatility, accuracy, and relatively low cost. Although initially developed for studies of stress and strain, large numbers are now used as sensing elements in the manufacture of other transducers.

Bonded strain gages were first manufactured of very fine resistance wire. Although such bonded wire strain gages are still in use, they have been largely superseded by the bonded metal-foil strain gage. Both operate on the same principle. When subjected to tension, the wire or foil filament elongates, with a resultant reduction in cross-sectional area. Since the resistivity of a given filament is a function of its length and cross-sectional area, both effects increase the resistance of the filament. When supported by a firm cement bond, the filament can also be compressed with opposite effects on its resistance.

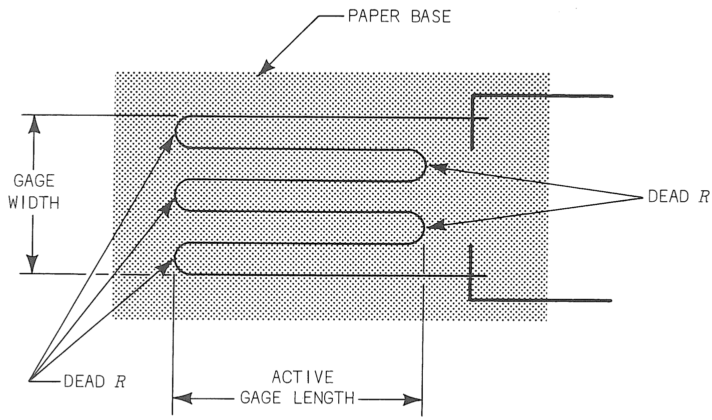


Fig. 6-1. Typical strain gage.

When the filament is folded to form a grid as in Fig. 6-1, small sections at the fold are not affected by tensional or compressive strains. This same *"dead resistance,"* however, is directly in line with Poisson strains. Since these strains are of opposite types, the "dead-resistance" change subtracts from the normal-resistance change. This effect is called *transverse sensitivity* and subtracts from the normal gage sensitivity. The manufacturer, however, tests samples of each gage lot on a calibrated test structure so that the effects of dead resistance are included in the published *gage factor*.

The majority of bonded resistance strain gages have a resistance of 120 Ω, but many other resistances are available. Gage factor for these types is nominally 2. The backing or gage-carrier is usually made of nitrocellulose paper, but bakelite is also used for higher-temperature gages.

Gage lengths vary from about 1/64" for the smallest metal foil gages to 6". Since strain is expressed $\frac{\Delta l}{l}$, it is clear that in actual measurements, the strain registered by a given gage represents the total elongation experienced by the gage *averaged over the length of the gage*. Thus, when strain is not evenly distributed in a member, the strain at any given point is most accurately determined by the *shortest* gage.

Many individual strain measurements require three strain gages, placed at different angles to a chosen axis. For convenience, rosette gages consisting of three gages mounted in one of several configurations on a common carrier are available from commercial sources (Fig. 6-2). Nomograms for quick solution of the strain problem are also available.

Where conventional temperature compensation techniques cannot be employed, it may be advisable to use a single temperature-compensated strain gage. These gages are designed to give compensation over a specific range and on a specific material.

Although strain gages will function at stresses beyond the yield point of most common materials, maximum strain should be kept within 2,000 $\mu\varepsilon$ for optimum repeatability and linearity. Linearity of most gages is on the order of 0.1 or 0.2%.

Semiconductor gages are characterized by their high gage factors, ranging from 50 to 250 and above. However, these gages suffer from a high degree of nonlinearity and require special circuitry if their full potential is to be realized.

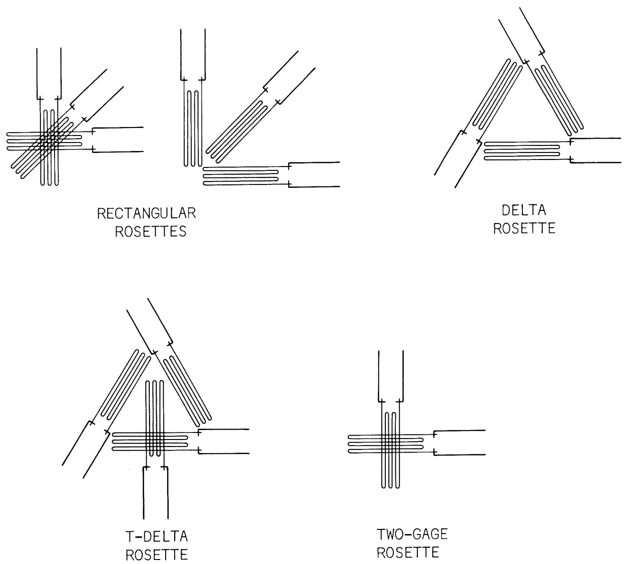


Fig. 6-2. Strain gage rosette configurations.

M-M **ENGINEERING DATA SHEET**

THE INFORMATION APPEARING ON THIS SHEET HAS BEEN COMPILED SPECIFICALLY FOR THE GAGES CONTAINED IN THIS PACKAGE. THIS FORM IS PRODUCED WITH ADVANCED EQUIPMENT & PROCEDURES WHICH PERMIT COMPREHENSIVE QUALITY ASSURANCE VERIFICATION OF ALL DATA SUPPLIED HEREIN. SHOULD ANY QUESTIONS ARISE RELATIVE TO THESE GAGES, PLEASE MENTION GAGE TYPE, ITEM NUMBER, AND LOT NUMBER.

ITEM ______
CODE ______
CHECK ______
FINAL QA ______

**MICRO-MEASUREMENTS**
**ROMULUS, MICHIGAN**
**PRECISION STRAIN GAGES**

M-M

EA-06-125BT-120

EA-06-125BT-120
GAGE TYPE

120.0 ± .15%
RESISTANCE IN OHMS

2.11 ± 0.5%
GAGE FACTOR AT 75° F

$K_t$: +0.6%

Q-A21AD06
LOT NUMBER

5 GAGES
QUANTITY

OPTIONS

## GENERAL INFORMATION: SERIES EA STRAIN GAGES

Form: B2-440
Code: 782121

APPLIES TO ALL LOT NUMBERS WITH THE PREFIX 'Q'

TEMPERATURE RANGE: Cryogenic to approximately +400°F for static measurements; to +500°F for dynamic strain.

SELF-TEMPERATURE-COMPENSATION: See data curve below.

STRAIN LIMITS: 30,000 to 50,000 microstrain (3% to 5%), tension or compression.

FATIGUE LIFE: Over $10^7$ cycles at ± 1400 microstrain; over $10^6$ cycles at ± 1500 microstrain or approximately 2800 microstrain unidirectional (tension or compression). Longer gage lengths and lower resistance gages show greater endurance.

CEMENTS: Particularly compatible with 'M-M' Certified Eastman 910 for fast installation. M-Bond 600 or RTC are recommended for long-term tests. M-Bond 610 is the best choice over the entire operating temperature range for elastic strains.

TEMPERATURE-INDUCED APPARENT STRAIN — LOT NO. A21AD06

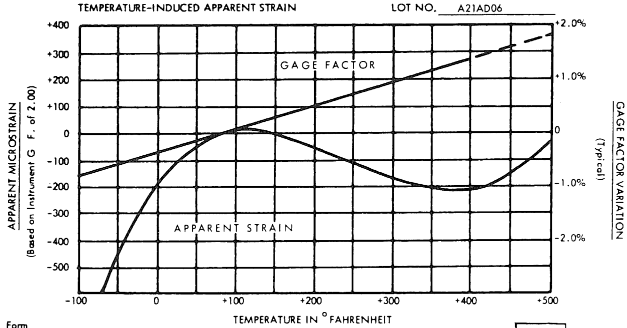


Form C1012-B — TESTED ON: 1018-STEEL — CODE: 792922 — Q.A.

TEST PROCEDURES USED BY MICRO-MEASUREMENTS FOR STRAIN GAGE PERFORMANCE EVALUATION

| | |
|---|---|
| OPTICAL DEFECT ANALYSIS: | M-M Procedures and Standards |
| GAGE FACTOR AT 75°F: | ASTM E251-67 (Constant Stress Cantilever Method)* |
| G. F. VARIATION WITH TEMP: | ASTM E251-67 (Step Deflection Method) |
| APPARENT STRAIN VS. TEMP: | ASTM E251-67 (Slow Heating Rate, Continuously Recorded) |
| TRANSVERSE SENSITIVITY: | ASTM E251-67 |
| INITIAL RESISTANCE: | M-M Procedure, Direct NBS Traceability on Resistance Standards |
| FATIGUE LIFE: | NAS 942 (Modified) |
| STRAIN LIMITS: | NAS 942 (Modified) |
| GAGE THICKNESS: | M-M Procedure |
| CREEP & DRIFT: | M-M Procedure (Similar to NAS 942 Method) |

Form B1-431
Code: 781016

*NOTE: This data is obtained in an uniaxial stress field with Poisson's ratio of approximately .285.

Fig. 6-3.

Most strain gages come packaged in sets of five; gages carrying the same *lot number* have common resistance values, gage factors and tolerances. To avoid complications and errors, all gages in a bridge should be from the same lot. An engineering data sheet is usually included in the package, providing the user with all the characteristics and parameters essential to proper installation and use (Fig. 6-3).

When an excitation voltage is applied to a strain gage, it dissipates power in the form of heat. The *power density* of a given gage's dissipation depends on its resistance and grid area and is expressed in watts/in$^2$. The excitation voltage must be chosen to keep power density within the limits imposed by the conditions of the test. Graphs are included in the Appendix showing the power density of common strain gages of various grid areas over a range of bridge voltages. An associated table indicates the power density limits for various materials on which the strain gage may be mounted, under static and dynamic conditions.

installing the strain gage

The strain gage cannot be used as a precision measuring device unless it is properly bonded to the member under test. The techniques involved in bonding and waterproofing strain gages have been developed to a fine art. Several excellent texts are available which include full treatments of these subjects and should be consulted in unusual applications. However, the following procedure has been used with success at Tektronix and is recommended for most common applications.

1. Lay out scribe lines for gage location on surface (Fig. 6-4).

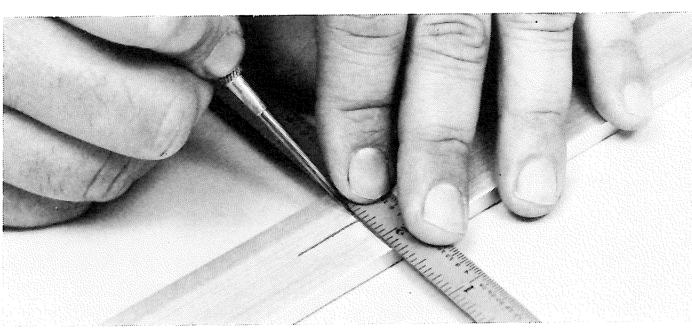

Fig. 6-4.

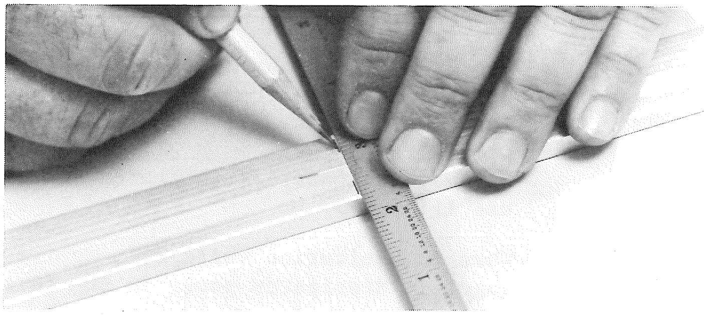

Fig. 6-5.

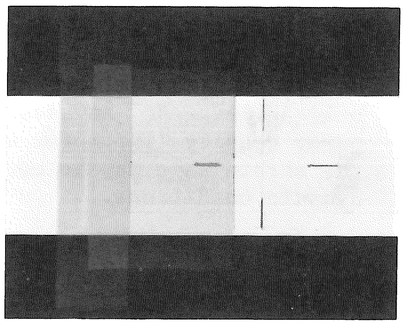

Fig. 6-6.

2. Sand with a 240 grit paper in a circular motion until scribe lines are barely visible.
3. Clean surface with solvent (alcohol, acetone or lacquer thinner) and mark in ends of scribe lines with hard pencil away from gage location (Fig. 6-5).
4. Line up gage on cross lines and mark location of lead end of gage.
5. Tape a piece of Mylar film across the above point to mask off the leads from the surface (Fig. 6-6). This prevents the leads from being glued down.
6. Clean the bottom of the gage.
7. Prepare the epoxy by squeezing out equal beads (about 1/2 inch long) of resin and hardener on a clean surface (i.e. paper) and mixing with a clean paddle until mixture is a uniform color.

NOTE: To check the epoxy, keep the paper it is mixed on. It should harden enough in 24 hours that a thin layer of it can be cracked by folding the paper. Eastman 910 contact cement may be substituted for faster installation.

8. With a clean paddle apply a thin coat of epoxy to the surface to wet it and a more liberal amount to the bottom of the gage.

9. Holding the gage by the leads with a pair of tweezers, place it on the surface and push it down into the epoxy with a soft instrument such as a pencil eraser and line it up with the scribed lines.

10. Place over the gage a strip of Mylar as shown and working through this strip roll out the excess epoxy from under the gage with a finger in the direction away from the leads (Fig. 6-7). When this is properly done, the gage will appear flat on the surface.

11. Once the gage is flat on the surface, it can be realigned with the scribed lines by pressing on the gage through the Mylar strip and moving the strip (both will act as one unit). When aligned, the Mylar is taped securely to the surface to prevent any more movement.

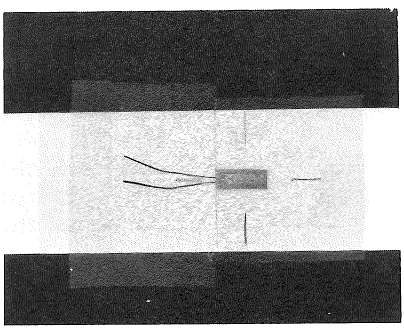

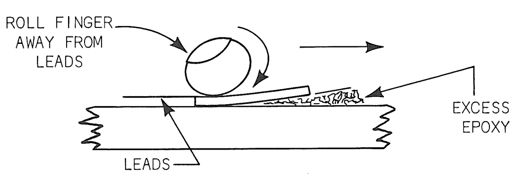


Fig. 6-7.

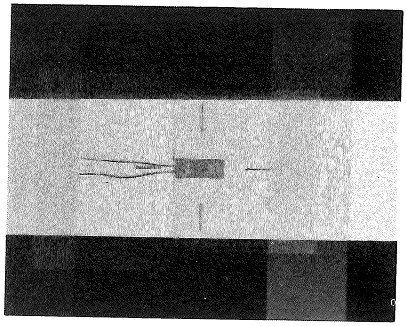

Fig. 6-8.

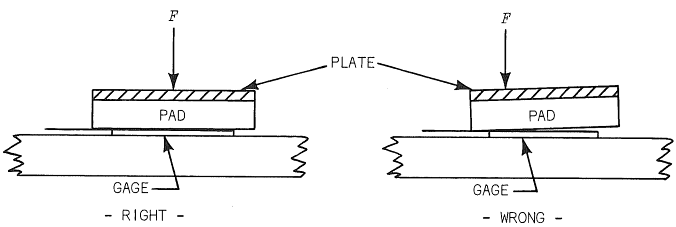


Fig. 6-9.

12. Now place another strip of Mylar over the gage and leads (Fig. 6-8) and place a neoprene pad and metal plate over the gage.

13. Apply a weight of approximately 5 to 10 pounds to the pad and plate making sure that the weight is centered on the plate so that the pressure on the gage is uniform (Fig. 6-9). One possible way to insure that the pressure on the gage is uniform is to apply the weight to the pad and plate as shown in Fig. 6-10.

14. After epoxy has set for at least 12 hours (wait at least 24 hours before use), carefully remove the weight, plate, pad and three Mylar strips.

15. Scrape off any excess epoxy from the area under the leads and rough up with sand paper.

16. Clean the area under the leads with solvent taking care not to get any on the strain gage.

17. Prepare the epoxy as before (Step 7).

    NOTE: Eastman 910 Contact Cement can be used also.

18. Wet the surface with a small amount of epoxy and apply a more liberal amount to the bottom of the terminal strip.

19. Push the strip down onto the surface and line up with the gage; keep the terminal strip close enough to the gage so that the leads from the gage to the strip can be looped (Fig. 6-11).

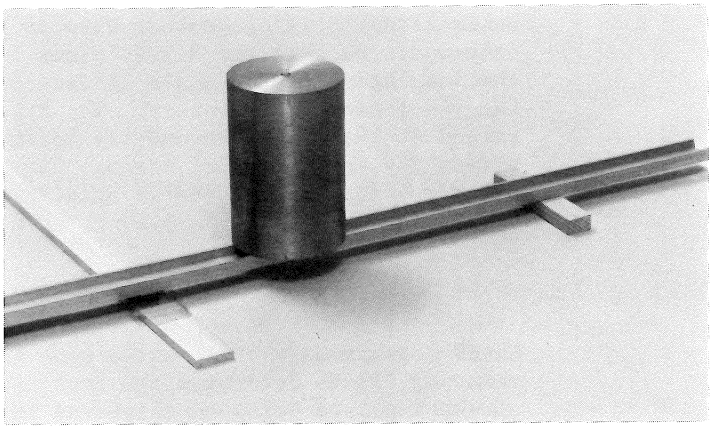

Fig. 6-10.

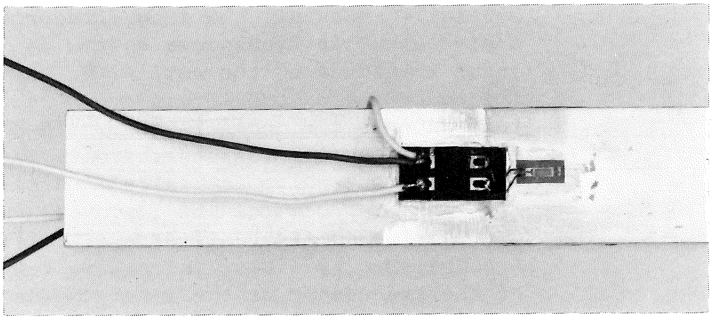

Fig. 6-11.

20. Allow about 12 hours for the strip to set on the surface and then solder the strain gage leads to the terminals. If 910 cement is used, the leads can be soldered immediately. (Leave a loop in the leads to prevent any strain at the connection on the gage.)

21. Solder the cable leads to the terminal. Connect cable to strain gage adapter.

22. The gage and strip may now be sealed, or coated with the R.T.V. (room temperature vulcanizing) Silicone Rubber Waterproofing Compound. Be sure the R.T.V. flows around the insulation of the cable leads. Clean the insulation if necessary. The R.T.V. should extend at least 1/4" beyond the edges of the strain gage and terminal strip. Further waterproofing information is printed on the R.T.V. tube.

## SHOCK MEASUREMENTS*

Shock measurements are usually made for one of two reasons; (1) to determine the amplitude and duration of shock pulses being administered to an object during drop-tests and similar aperiodic acceleration studies, or (2) to observe the mechanical response of an object when subjected to various conditions of shock.

Generally speaking, the lower-frequency response of a piezoelectric transducer system is limited by the input impedance of the amplifier, while the upper frequency limit is determined by the first mechanical resonance of the accelerometer. In shock studies, the low-frequency response becomes most important as the transient pulse increases in duration. Low-frequency response can be improved by increasing the RC time constant of the system. This can be accomplished by either increasing the capacitance of the transducer or the input impedance of the amplifier or both.

*Derived from "Shock and Vibration Measurements" Columbia Research Laboratories, Inc., 1970.

| PULSE SHAPE | $\frac{RC}{t}$ FOR 2% ACCURACY | $\frac{RC}{t}$ FOR 5% ACCURACY |
|---|---|---|
|  HALF SINE | 16 | 7 |
| 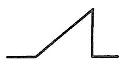 SAWTOOTH | 16 | 7 |
| 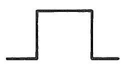 SQUARE | 50 | 20 |

Table 6-1. *RC* requirements for three common pulse shapes.

The RC requirements for three common pulse shapes are shown in Table 6-1. The square pulse represents the worst case for the system. Any system which will handle a square pulse of a given duration $t$ will handle any type of transient of the same duration. Since the accelerometer associated with the 3A10 system has a capacitance of 10,000 pF and the amplifier has a 10 MΩ input impedance, the RC time constant (ignoring cable capacity and the amplifier's input capacity) is 0.1 seconds. Thus, square pulses up to 2 milliseconds in duration can be measured with 2% accuracy and up to 5 milliseconds with 5% accuracy.

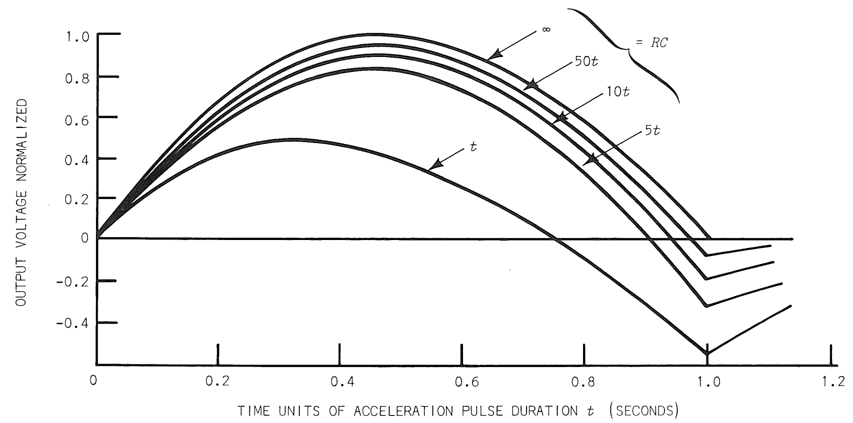


Fig. 6-12. Response of a piezoelectric accelerometer to a half-sine acceleration pulse for different RC times.

| $\frac{\text{INDICATED UNDERSHOOT}}{\text{INDICATED PEAK}}$ | $\frac{\text{ACTUAL PEAK}}{\text{INDICATED PEAK}}$ | APPROX $\frac{RC}{t}$ |
|---|---|---|
| 5% | 1.04 | 9 |
| 10% | 1.06 | 6 |
| 15% | 1.08 | 4 |
| 20% | 1.11 | 3 |
| 25% | 1.15 | 2.1 |
| 30% | 1.19 | 1.7 |
| 35% | 1.21 | 1.5 |
| 40% | 1.25 | 1.3 |
| 45% | 1.28 | 1.2 |
| 50% | 1.32 | 1.0 |
| 100% | 1.90 | 0.4 |

Table 6-2. Undershoot or degree of error in driving a half-sine pulse through an *RC* network.

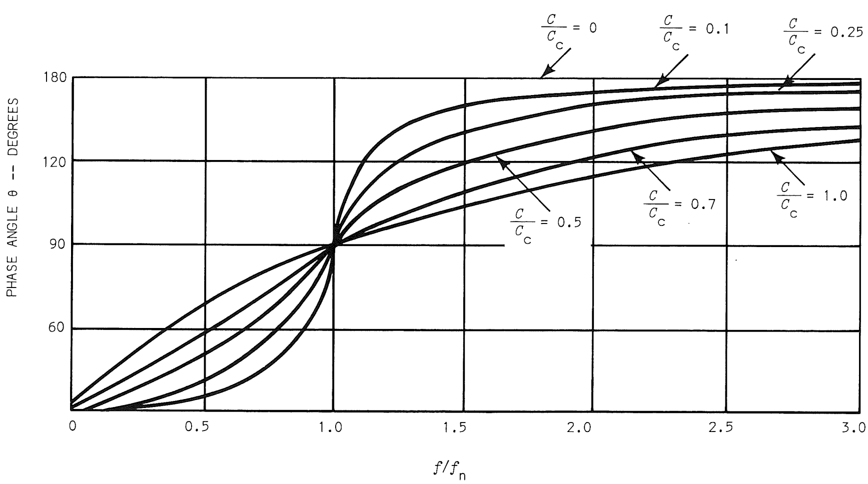


Fig. 6-13. Phase angles versus ratio of forcing to natural frequency.

Typical half-sine pulses react to inadequate $\frac{RC}{t}$ ratios by losing amplitude and exhibiting undershoot, as shown in Fig. 6-12. The five curves show that the accelerometer output exhibits a negative overshoot when the pulse returns to zero. Table 6-2 lists the correction factors which should be applied when such a spurious undershoot is observed at the termination of the pulse. It should be noted that for small undershoots, the required correction for peak values is roughly one-half the undershoot.

The time-constant of the system may be increased by shunting the accelerometer with a capacitor. It should be noted, however, that the sensitivity of the transducer will be decreased by the same ratio as the capacitance is increased.

amplitude response

Due to the mechanical response characteristics of piezoelectric accelerometers, the amplitude and phase of the output varies with frequency. See Chapter 3, "Acceleration." Considering the transducer as a single-degree-of-freedom system without damping,

$$\frac{\text{actual peak}}{\text{indicated peak}} = \frac{1}{1 - (f/f_n)^2}$$

where $f$ = operating or forcing frequency and

$f_n$ = natural frequency

At the recommended $f/f_n$ ratio of 1/5, the sensitivity is 1.04 or about 4% high. This figure can be improved, however, with proper damping. The same is true of shifts in phase angle. Fig. 6-13 shows the effects of damping on phase angle of the output for various coefficients of critical damping.

It is customary for manufacturers to supply correction tables for sensitivity and phase angle with the transducer.

## APPLICATION: DIE-CASTING MACHINE

The purpose of this investigation was to monitor the operation of an aluminum die-casting machine to determine the nature and magnitude of various mechanical forces critical to its proper performance.

The die-casting machine (Fig. 6-14) is an apparatus which allows the casting of aluminum parts to precise dimensions, which cannot be achieved by older mold-casting methods. The die itself consists of two heavy blocks of special alloy steel, machined to form a mold for the molten aluminum. In operation, the two halves of the die are brought together under tremendous pressure to assure complete closure. Molten aluminum at about 1200°F is then injected into the die by a hydraulic ram, driving the molten metal into the small orfices and crevices in the die under very high pressure. Although the dies themselves are heated to about 500°F, the metal quickly solidifies. The casting or "biscuit" is then given a sharp "kick" to loosen it from the die. Then the halves of the die are separated and the casting is removed from the mold. After the die faces have been inspected and lubricated, the cycle is repeated. The entire cycle takes only a few seconds, so that one man can turn out large numbers of castings in a normal working day.

The force holding the dies in contact must be maintained at the proper level to assure absolute integrity of the mold. When this contact is not achieved, the molten aluminum may be ejected from the mold interface at very high velocities, sufficient to pit a concrete wall over 15 feet away. The operator is protected by a heavy sliding safety door. Closure of the door actuates a switch in the control circuit of the machine so that injection cannot be accomplished when the door is open.

Three measurements were made on this machine. To determine the closing force exerted on the dies, strain gages were mounted on one of the four 6" diameter tie bars as shown in Fig. 6-15. A heavy casting called the stationary platen carrying the die-closing mechanism is clamped to the tie bars. All the die-closing force is thus communicated to the tie bars by the platen, setting up tensional strains in the tie bars. By measuring these strains, the stress in the tie bars can be determined, and from these values the actual force applied to each shaft can be calculated.

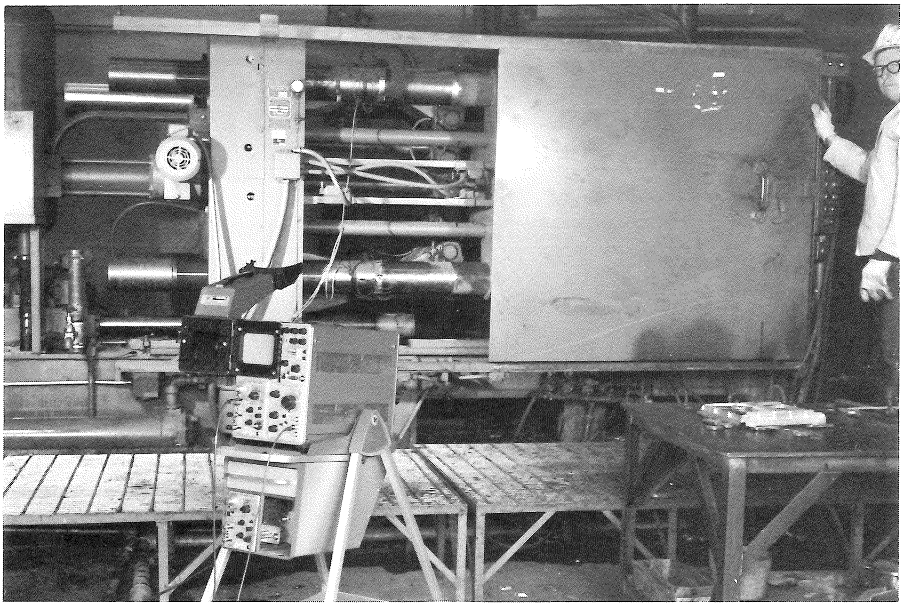

Fig. 6-14.

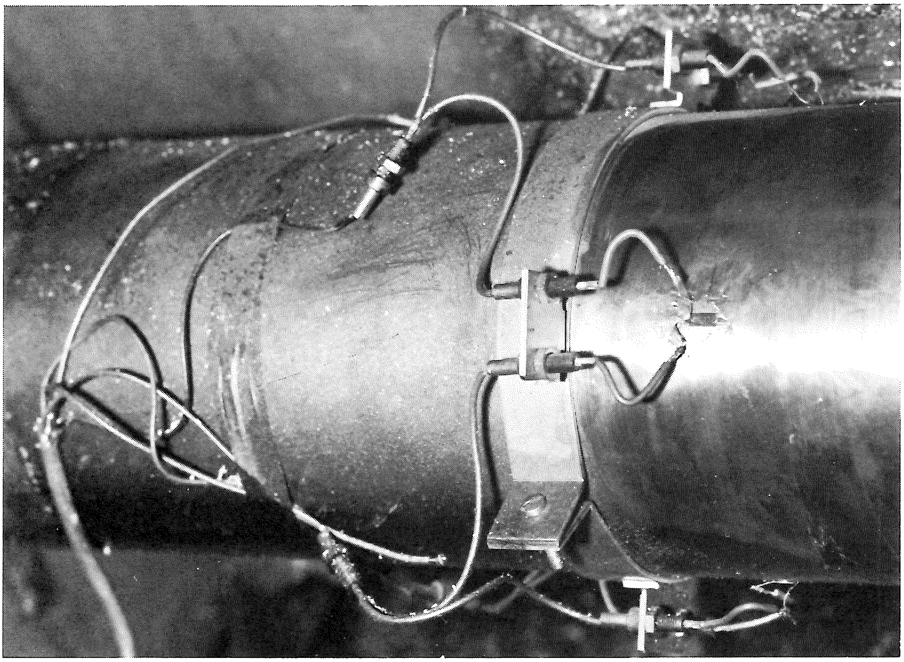

Fig. 6-15.

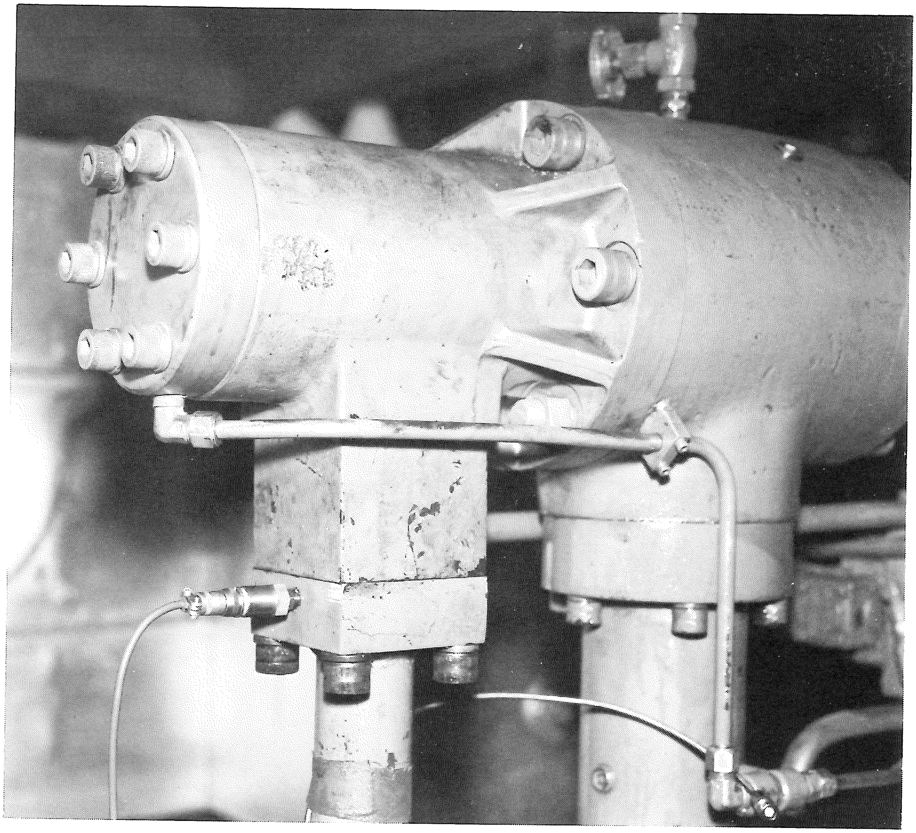

Fig. 6-16.

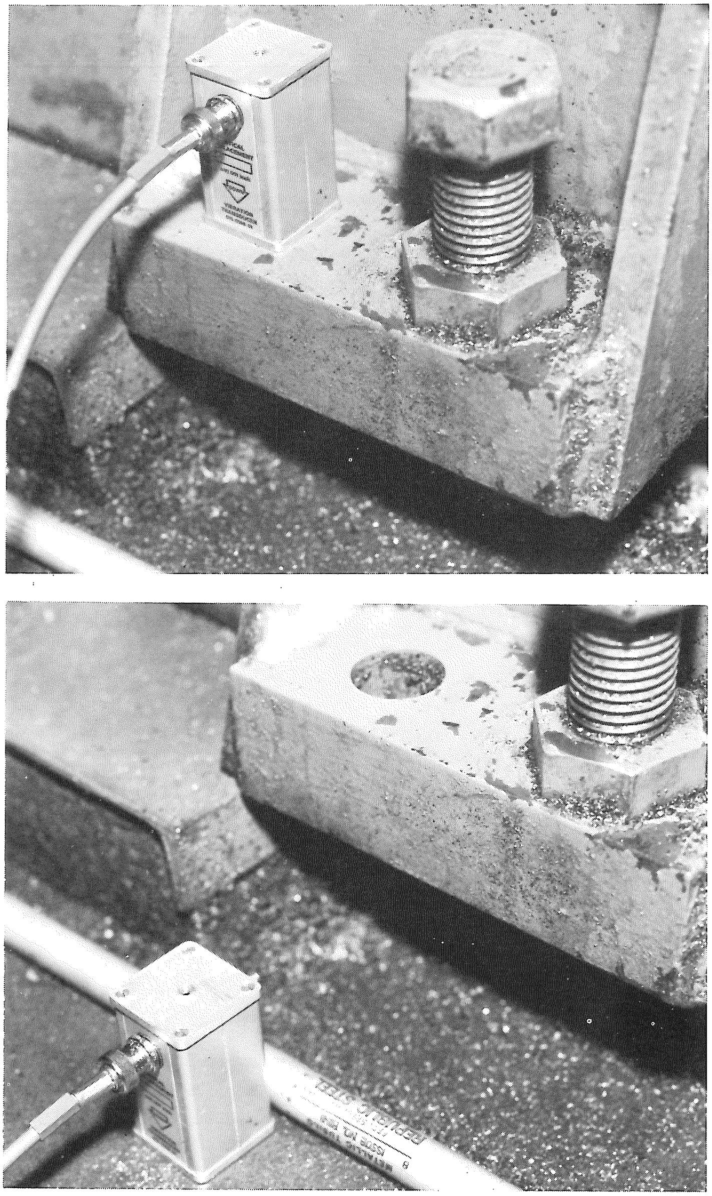

Fig. 6-17.

The hydraulic pressure exerted on the injection ram was measured by inserting a 3,000 pound pressure transducer in the hydraulic cylinder (Fig. 6-16). Vibration measurements were also taken at the base of the machine and from the floor closely adjacent, to determine the effectiveness of the shock mounting (Fig. 6-17).

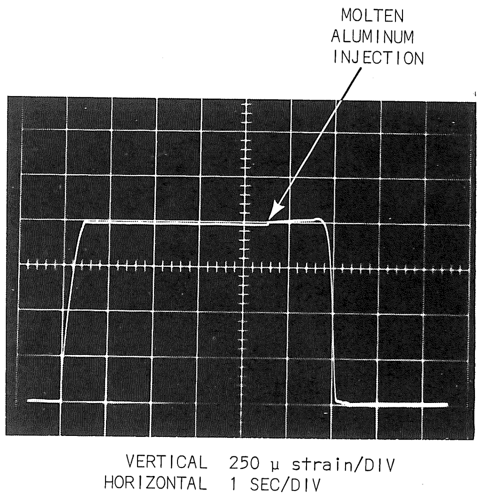


Fig. 6-18.

The results of the strain measurement are shown in Fig. 6-18. The oscilloscope was triggered by the closing of the safety door switch. The leading edge of the pulse shows the sharp rise in strain communicated to one of the tie bars by the closing of the die. The slight "bump" at the end of the upper portion of the waveform is caused by the injection of the molten aluminum into the die. The trailing edge, of course, occurs as the mechanism separates the die halves and returns to the retract position.

Since four strain gages were mounted on the tie bar, the oscilloscope reading must be modified to reflect the true value of tensional strain. Fig. 6-19 shows the actual arrangement of the strain gages. Gages 1 and 3 were placed on opposite sides of the bar in line with the longitudinal axis to measure tensional strain. Gages 2 and 4 were placed at right angles to the longitudinal axis to measure Poisson strain. This arrangement provided an increased output, cancellation of any bending strain, and also temperature compensation.

Since the Poisson ratio of steel is about 0.3, the Poisson strains have a magnitude only 0.3 times that of the tensional strains. Thus the bridge will provide an output only 2.6 times that of a single gage measuring tensional strain. Also, since the total die-closing force is distributed between the four tie bars, the equation for the total force applied to the dies is:

$$F_t = 4\pi r^2 \sigma$$

$$= 4\pi r^2 E\varepsilon \quad \text{(from Equation 3-1)}$$

where $\varepsilon$ = oscilloscope strain reading

$r$ = radius of one tie bar

Therefore, taking the highest strain amplitude of 1100 μstrains shown by the waveform,

$$F_t = 4 \times 3.14 \times 3^2 \times (30 \times 10^6) \times \frac{(1100 \times 10^{-6})}{2.6}$$

$$= 14{,}500 \text{ lbs.}$$

$$= 7.25 \text{ tons}$$

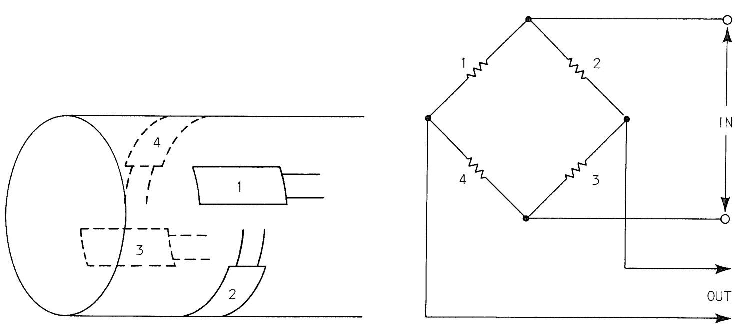


Fig. 6-19.

The pressure waveform (Fig. 6-20) is triggered by the switch which activates the injection ram. The hydraulic end of the ram has an area of 10 $in^2$, while the metal-injection end has an area of 2.5 $in^2$. Therefore, the metal-injection pressure exceeds the hydraulic pressure by a factor of 4. The waveform indicates that the hydraulic pressure initially peaked at 1380 $lbs/in^2$ and showed a steady-state pressure of about 840 $lbs/in^2$. Metal-injection pressure was therefore 5520 $lbs/in^2$ and 3360 $lbs/in^2$ respectively.

The vibration waveforms shown in Fig. 6-21 were also triggered by the injection initiation switch and cover a full cycle of machine operation. The peaks occur during the time of injection and later during the die closing operation. Since the displacement output of the vibration transducer was used, the peak vibration displacement at the machine base was about 0.0076". The floor vibration, however, peaked at a maximum of 0.00064", indicating that the shock mounting effectively damped out the machine vibration by a factor of about 10.

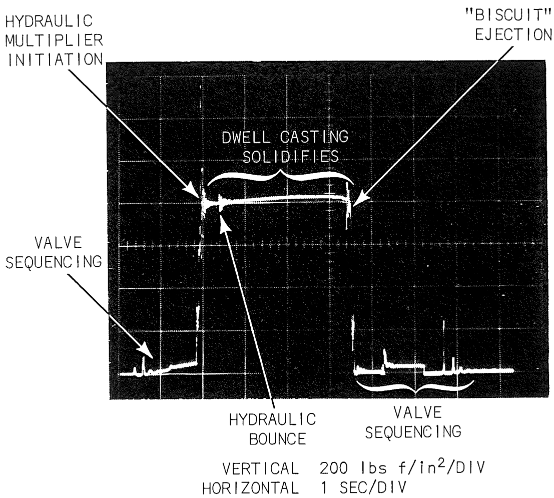


Fig. 6-20.

Waveforms such as those in Fig. 6-21 are highly useful in locating areas of malfunction when the die-casting machine fails to perform satisfactorily. In fact, in taking these photographs, the presence of air in the hydraulic system was immediately revealed when the "bump" on the strain waveform in Fig. 18 began to disappear. Normal operation was restored by bleeding off the trapped air.

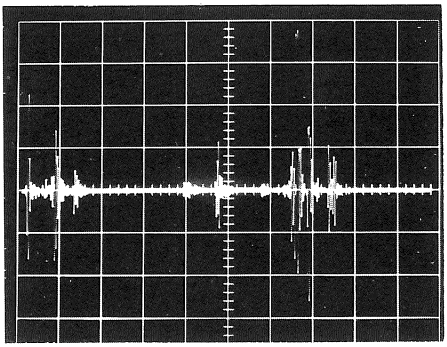

VERTICAL $2 \times 10^{-3}$ inch/DIV
HORIZONTAL 2 SEC/DIV

(A)

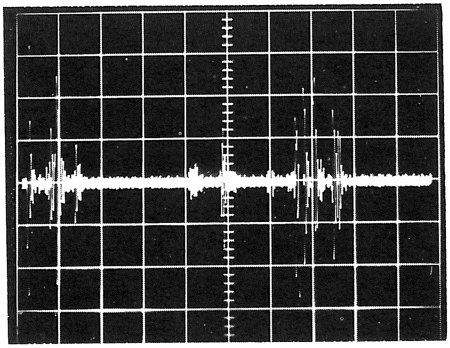

VERTICAL $0.2 \times 10^{-3}$ inch/DIV
HORIZONTAL 2 SEC/DIV

(B)

Fig. 6-21.

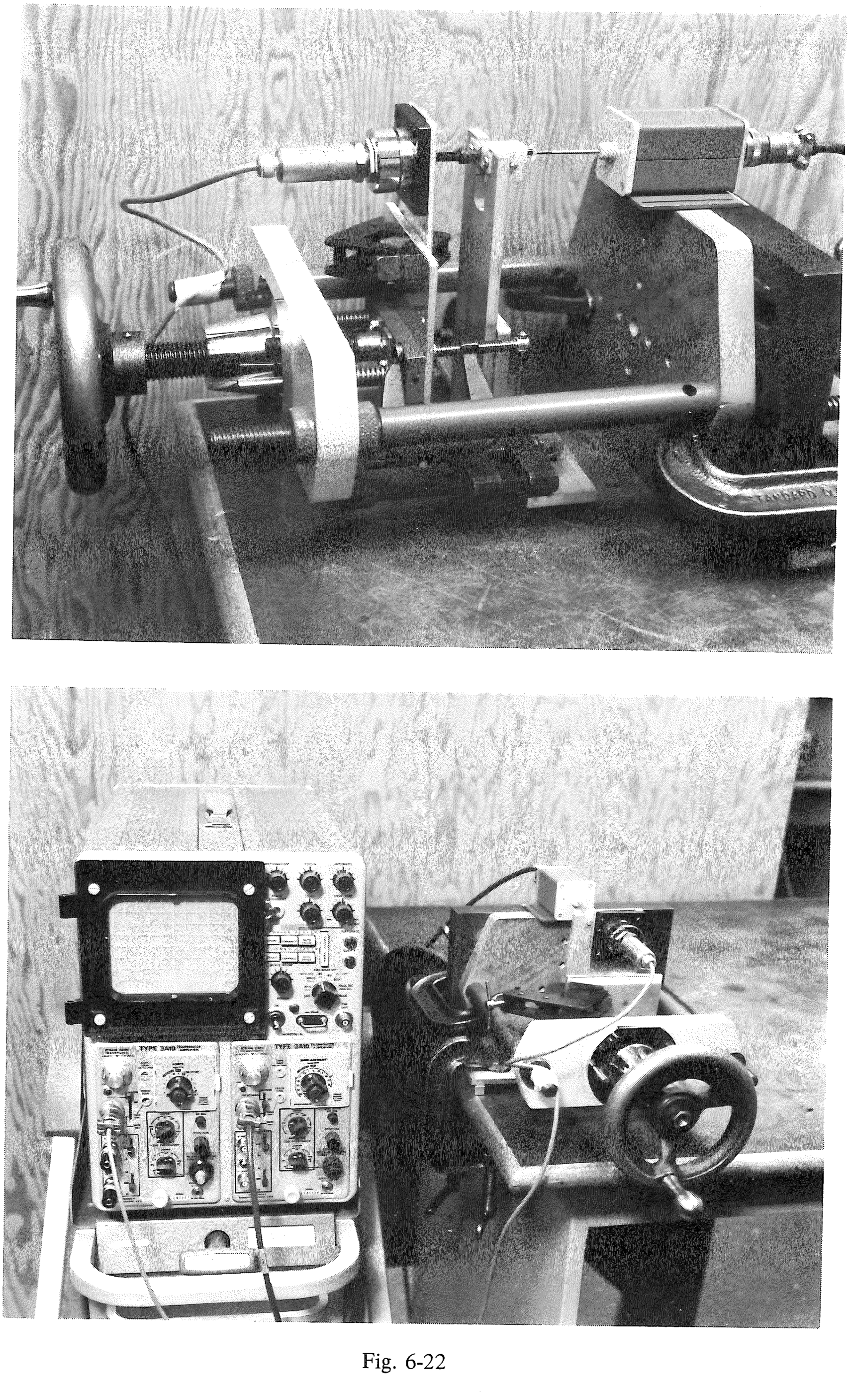


Fig. 6-22

APPLICATION: PUSHBUTTON SWITCH

It is highly important in designing an instrument to obtain a clear picture of the behavior of its mechanical components. In many cases it is not possible to rely on unaided sensory perceptions in obtaining this knowledge. Sensitive transducers can often give a clear picture of small events that would ordinarily go undetected. In this application the behaviour of a small plastic double-acting pushbutton switch was examined by making a plot of actuating force versus pushbutton displacement. A jig was improvised from a small press, using scraps of aluminum and several clamps (Fig. 6-22). The displacement transducer was bonded to the press frame with double adhesive tape. The 50 pound-force transducer was mounted in the same fashion on a metal strip clamped to the pressure plate. The switch itself was screwed to a third plate clamped to the bench. The press was also clamped to the bench. By turning the hand wheel of the press the force transducer was brought to bear on the switch-actuating pushbutton. Motion of the pushbutton was transmitted to the extension rod of the displacement transducer. Contact was maintained through another small piece of double adhesive tape.

Two 3A10 transducer amplifiers were used in a 564B oscilloscope, used in the storage mode. The displacement transducer output was applied to the right hand amplifier to provide horizontal displacement of the CRT electron beam. The force transducer was connected to the vertical amplifier.

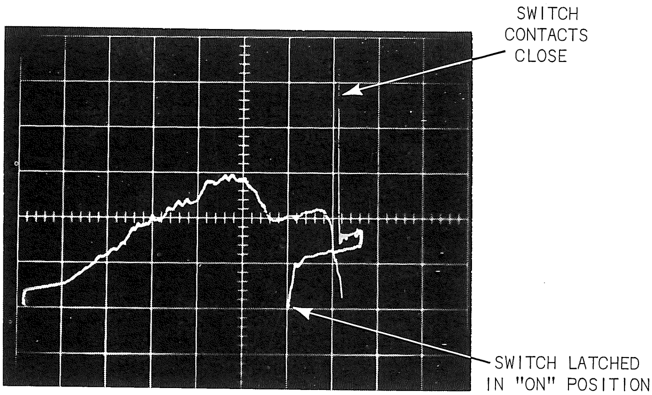


Fig. 6-23.

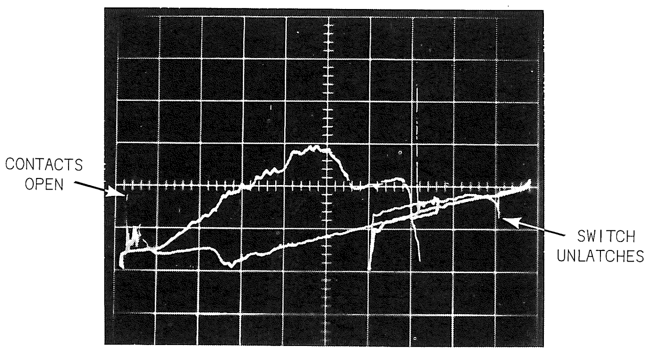


Fig. 6-24.

The recorded waveform reveals a number of interesting details of the switch's operation. In Fig. 6-23, as the hand wheel is rotated, the force applied to the switch rises abruptly until it overcomes the friction of the switch mechanism. Then for a period, the increase of force with displacement forms a fairly linear pattern, although small aberrations in the waveform indicate "stick-slip" operation. Where the force begins to drop off, the switch spring has reached the linear portion of the cam and is about ready to snap the contacts together. Just before the snap, force on the switch has dropped almost to zero. The actual contact closure administers a sharp impulse of force to the transducer and occurs so rapidly that only a faint trace appears on the CRT screen.

As the hand wheel is rotated in the opposite direction, the pushbutton retracts, eventually returning to its "cocked" or "on" position with the contacts closed. Fig. 6-24 shows the completed cycle waveform. To unlatch the switch, it is first pushed forward until the latching spring is forced off the cam. The small negative spike at the ninth horizontal division line reflects this event. The return to the "off" position of the switch is quite linear, falling almost to zero force until the opening action of the switch contact spring is initiated. Another sharp pulse near the origin of the waveform shows the actual opening of the contacts.

The switch used in this demonstration would be rejected due to the rough spring action noted above, probably caused by irregularities in the switch cam.

APPLICATION: DROP TEST

Drop tests are performed to administer shock pulses of known magnitude and duration to an object or instrument and usually are encountered as part of any comprehensive environmental testing program.

A typical drop test setup is shown in Fig. 6-25. An accelerometer is mounted on a drop table which supports the instrument under test. The drop table is raised by an electrically driven mechanism to the desired height, then allowed to drop in free fall. As it hits bottom, a shock pulse is applied to the test instrument. The pulse is communicated to the oscilloscope by the transducer. The amplitude, shape and duration of the pulse are controlled by varying the height of the drop and by using cushioning materials of various thicknesses and compositions to soften the table's fall. The instrument may be subjected to pulses of increasing amplitude or shorter duration, until something "gives," in order to establish the limits of abuse it will tolerate, or may be subjected to a specified program of shock events to prove its ability to tolerate rough handling. For example, the National Safe Transit Committee publishes a program designed to simulate actual truck shipment conditions over various trip mileages. Such tests are highly useful in designing adequate packaging and safe containers for fragile shipments.

In this application the drop table was raised to a height of 6 inches and its fall was cushioned by two layers of 3/4 inch rubber. A vertical vibration transducer was fixed to the floor to register the vibration induced by the action of the drop table.

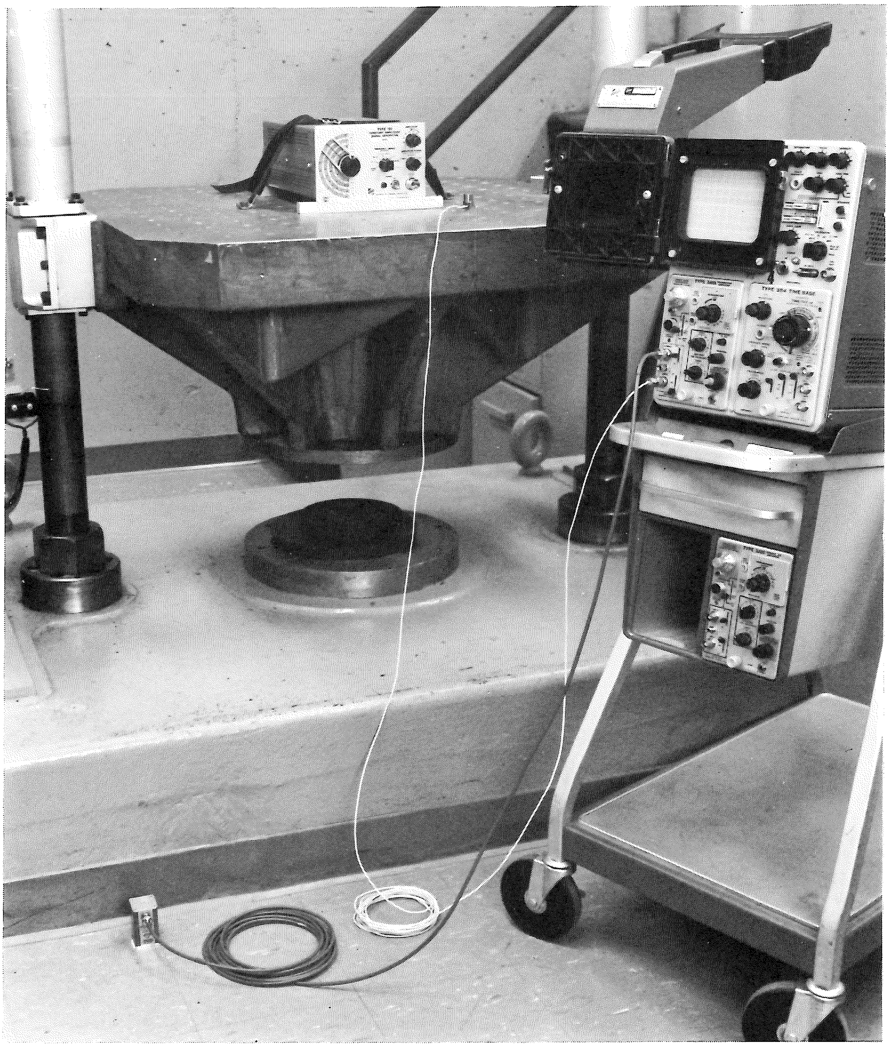

Fig. 6-25.

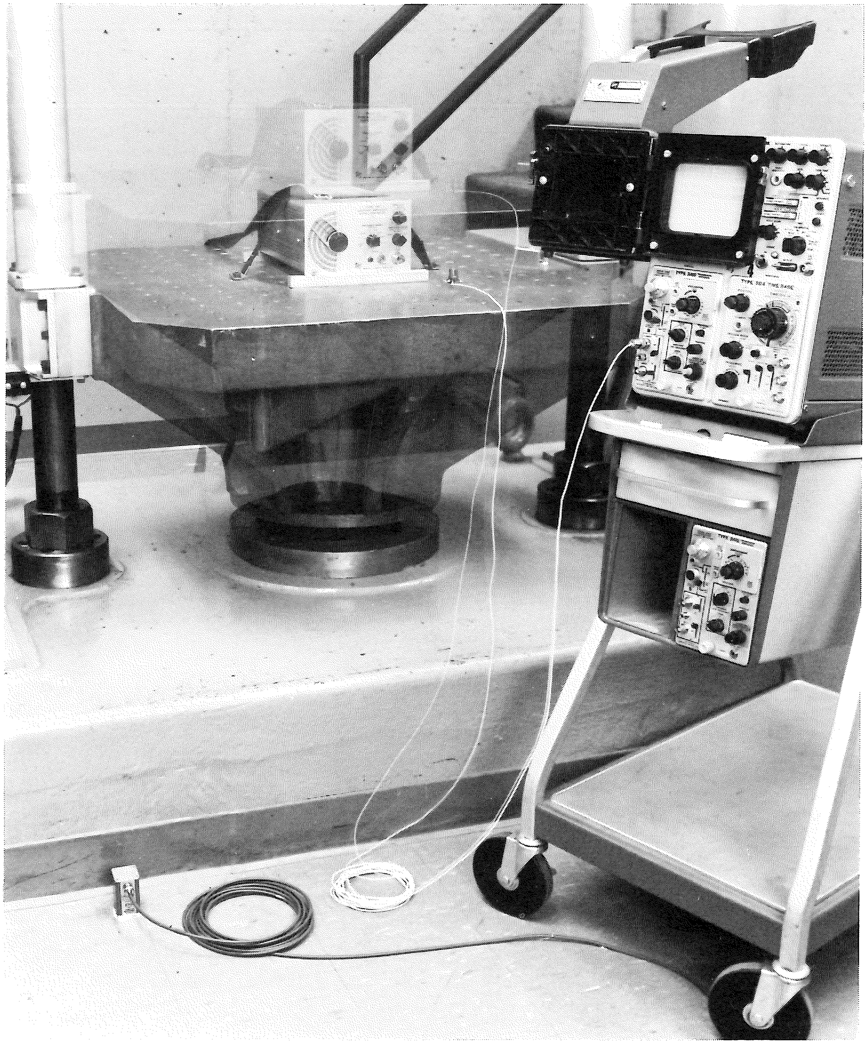

Fig. 6-26.

The instrument under test was mounted on metal bars (so that its rubber supporting feet could not cushion the administered shock) and strapped down firmly to the table. When the table was dropped (Fig. 6-26), the waveform shown in Fig. 6-27 was produced. After correcting the pulse amplitude by one-half the undershoot as explained earlier in this chapter, a peak acceleration of about 42.5 g's was attained by the 6 inch drop. Duration of the pulse, measured from origin to the first negative peak, was 16 milliseconds.

The vibration waveform (Fig. 6-28) was triggered by the unlatching mechanism of the drop table. It shows the vibration displacement caused by the first impact and two successive bounces of the table on the rubber cushioning. As shown by the low frequency (about 20 Hz) and extremely low amplitude (about 0.00035" max) of the vibration cycles, very little shock was communicated to the floor by the dropping of the table.

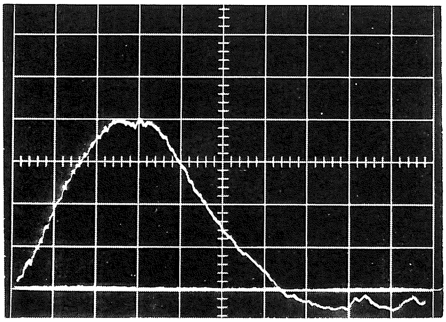

VERTICAL 10 g/DIV
HORIZONTAL 2 mSEC/DIV

Fig. 6-27.

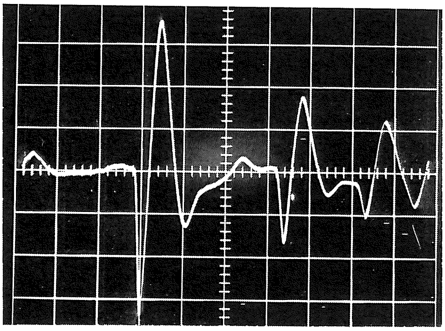

VERTICAL $0.1 \times 10^{-3}$ inch/DIV
HORIZONTAL 50 mSEC/DIV

Fig. 6-28.

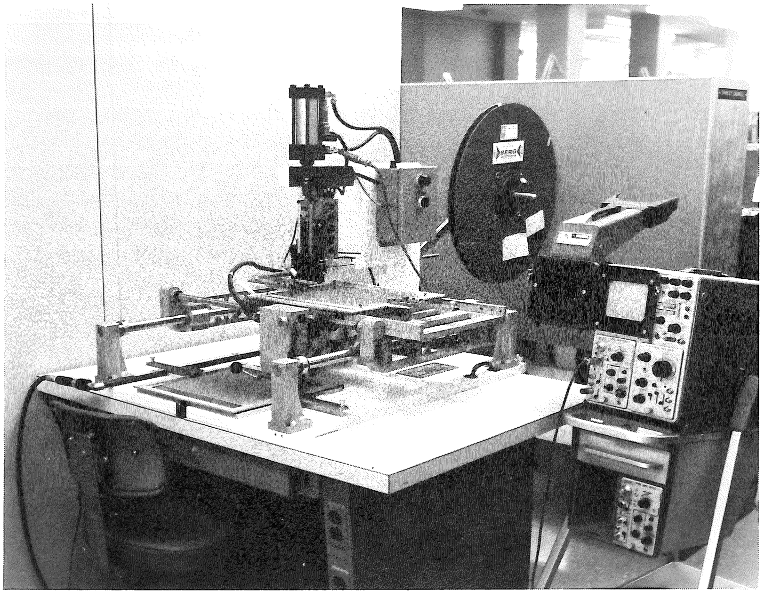

Fig. 6-29.

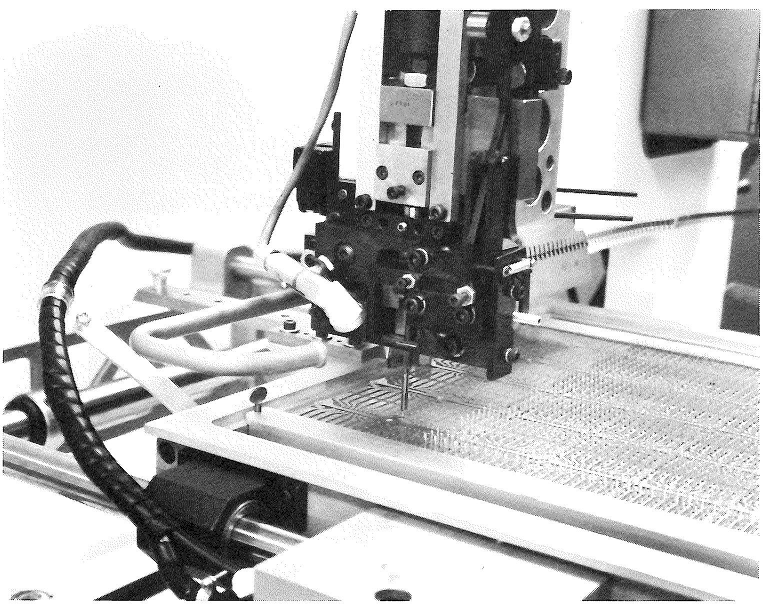

Fig. 6-30.

APPLICATION: PNEUMATIC PRESSURE TEST

Many industrial processes are performed by machines which are both powered and controlled by pneumatic pressure. In this application the operation of a pneumatic pin-setting machine (Fig. 6-29), used to insert wiring-terminal pins in etched-circuit boards, was examined. The most convenient access point proved to be on the under side of the header piston. This piston drives the pin into the board when pressure is applied to the upper side of the piston and the lower side is vented to the atmosphere (Fig. 6-30). At the conclusion of its power stroke, the header is retracted by pressure applied to the under side of the piston and venting of the upper side.

The waveform shown in Fig. 6-31 reveals the sequence of events as the machine was put through one cycle of operation. When the control valve vents the lower side of the piston to the atmosphere(1), the pressure drops rapidly at first. Since the piston is being forced down by pressure on its upper half, however, the pressure in the lower half levels off at about 8 $lbs/in^2$(2) until the piston reaches the end of its stroke(3). Then the remaining pressure bleeds rapidly off until it is in equilibrium with the atmosphere(4). As the control valve reverses, pressure rises rapidly before the piston can move(5), then levels off(6) as the piston returns to its retracted position(7). Finally, the curve climbs slowly as cylinder and operating pressure come to equilibrium at about 76 $lbs/in^2$.

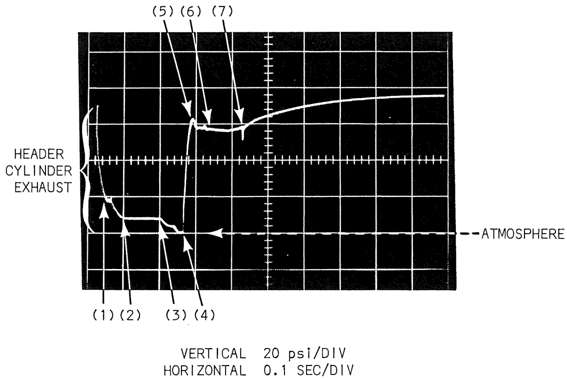


Fig. 6-31.

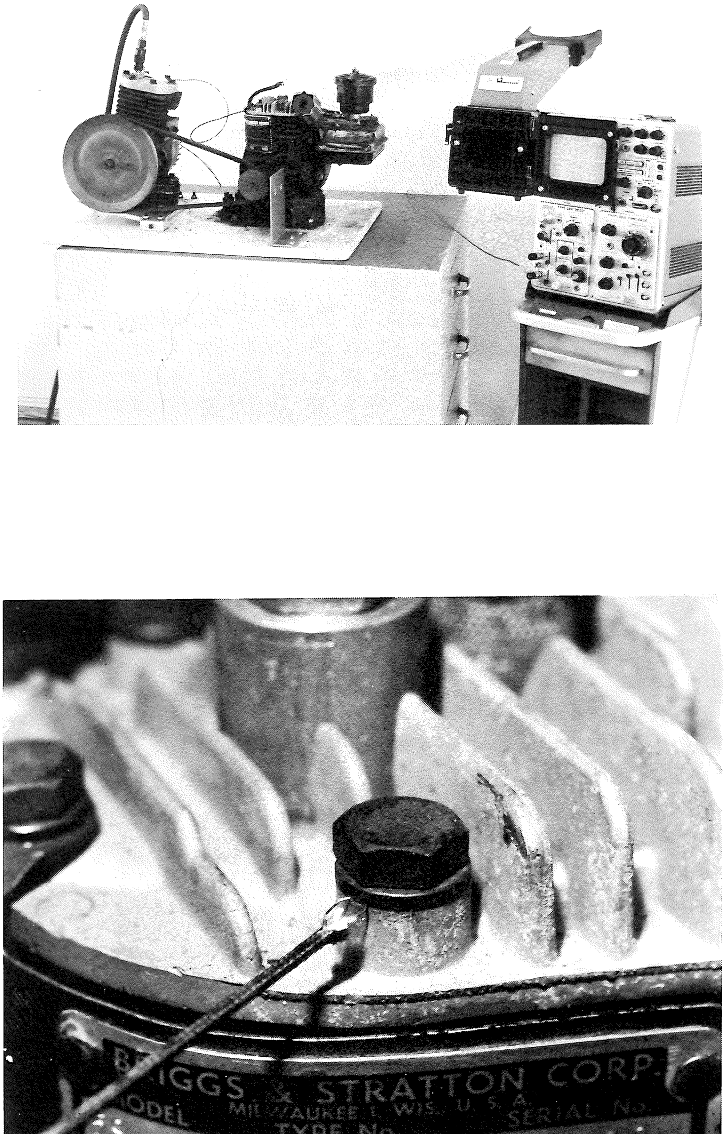


Fig. 6-33.

By comparing waveforms of this kind with the sequence of events normally performed in the operation of the machine, malfunctions may be quickly identified and located, with a consequent savings in time and labor.

## APPLICATION: PRESSURE-TEMPERATURE VARIATIONS IN A COMPRESSOR

A small, home-assembled compressor, driven by a lawnmower-type gasoline engine (Fig. 6-32), provided some interesting data in this application. Interest was centered on temperature variations of the engine's cylinder head, as well as pressure and temperature variations in the compressor itself.

To measure cylinder-head temperature variations, the 20-foot glass-braid thermocouple was first inserted under one of the cylinder head bolts (Fig. 6-33). When the engine was started, the DC level of the resulting waveforms climbed rapidly, showing that the thermocouple was reacting properly to the changing temperature. However, at the 20-microvolt sensitivity setting necessary to show temperature variations of the cylinder head to the internal combustion, differences in the conductivity of the two thermocouple materials was sufficient to cause pickup of the ignition voltage even though the amplifier was used in the differential mode (see Fig. 6-34). Interpretation of the waveform as a temperature signal, therefore, could not be made.

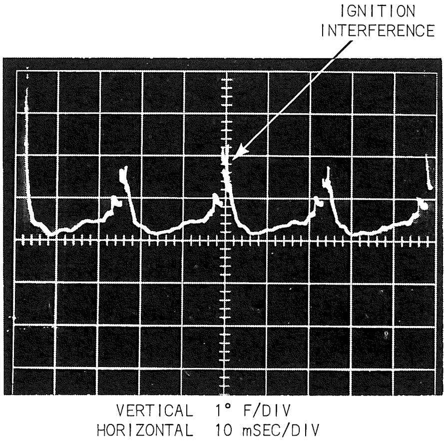


Fig. 6-34.

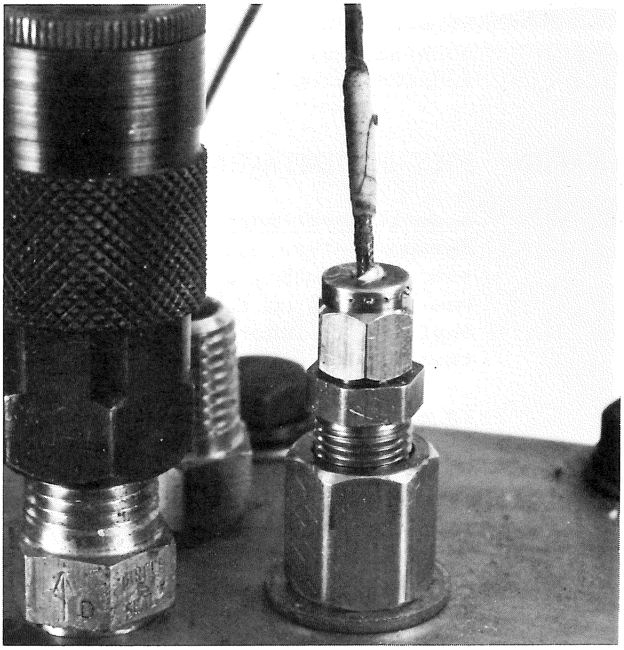

Fig. 6-35.

Much more satisfying results were obtained in measuring the temperature variations in the compressor. Here the thermocouple was inserted through a packing gland directly into the compression chamber (Fig. 6-35). The compressor was loaded by controlling the escape of air from the pressure outlet. Variations in air temperature within the compression chamber as cool air was drawn in then compressed by the compressor piston are clearly shown by the waveform in Fig. 6-36.

Pressure measurements were also made at the same location to show the relationship between the two quantities. Fig. 6-37 shows the waveform obtained. Note the slight aberrations at the waveform peaks, due to opening and closing of the pressure valve and subsequent opening of the intake check valve. Closing of the intake valve also produced a slight oscillation in the waveform at the beginning of the pressure stroke.

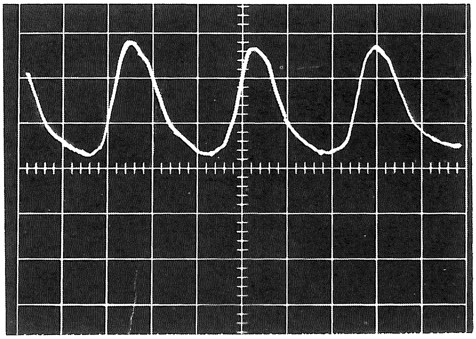


Fig. 6-36.

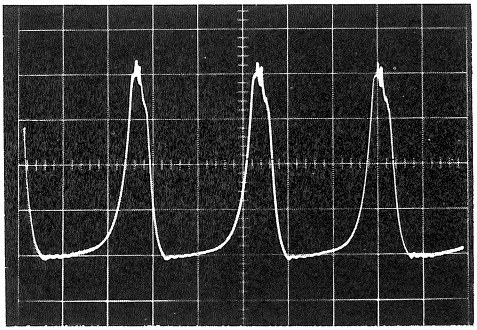


Fig. 6-37.

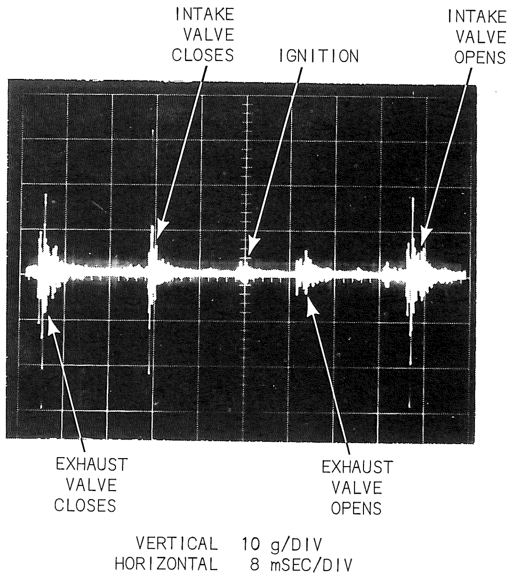


Fig. 6-38.

An accelerometer attached to the cylinder head of the 4-cycle engine provided the vibration waveform shown in Fig. 6-38. The lower bandwidth switch on the 3A10 was placed in the 10 kHz position to eliminate low-frequency vibrations. The high-frequency vibration remaining is due primarily to gas turbulence within the cylinder on intake and exhaust and valves hitting the seats. Note the relatively low amplitude of this vibration on the power stroke. This indicates that the valves and rings were in good condition, allowing very little leakage at the valve seats or "blow-by" (gas leakage past the piston rings during the power stroke).

## APPLICATION: SHAKE-TABLE EXPERIMENT

This application demonstrates the versatility of a transducer system as a classroom training aid. The objective, in this instance, was to provide graphic evidence of the mathematical relationship between various dimensions of motion (see Chapter 3). The apparatus shown in Fig. 6-39 consists of a small shake table, upon which are mounted a vertical vibration transducer and an accelerometer. A 60-Hz squarewave voltage was applied to the shake table.

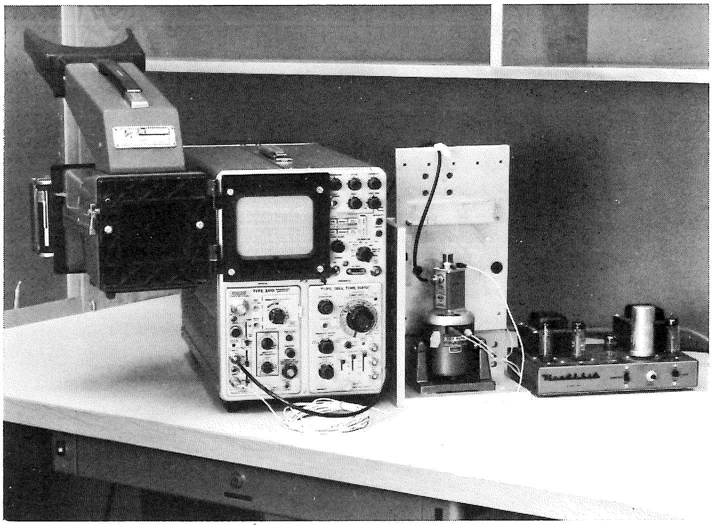

Fig. 6-39.

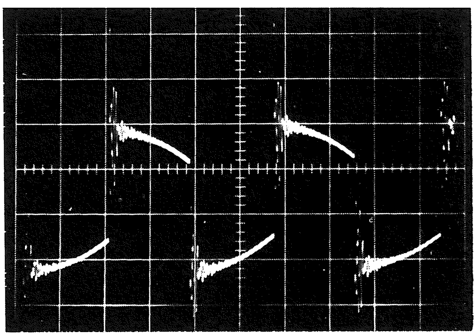

VERTICAL 2 mV/DIV
HORIZONTAL 2 mSEC/DIV
BANDWIDTH DC TO 1 MHz

Fig. 6-40.

The first measurement taken was that of acceleration. The output of the accelerometer was applied to the 3A10 amplifier, adjusted for maximum bandwidth. The resulting waveform is shown in Fig. 6-40. This waveform should represent the first derivative of the vibration velocity, and the second derivative of the vibration displacement, both with respect to time.

Fig. 6-41 shows the same waveform, but with the high-frequency components attenuated by reducing the upper bandwidth limit of the 3A10 to 3 kHz.

The next measurement taken was of vibration velocity (Fig. 6-42). For this measurement the bandwidth was again adjusted to maximum. It can be shown without much difficulty that the resulting waveform is a fairly accurate representation of the integration of the acceleration waveform in Fig. 6-41. To reinforce this contention, the velocity waveform was differentiated by raising the lower bandwidth limit to 10 kHz, yielding the curve shown in Fig. 6-43. Although considerable attenuation of the signal occurs in this procedure, the resemblance between Fig. 6-43 and Fig. 6-41 is unmistakable.

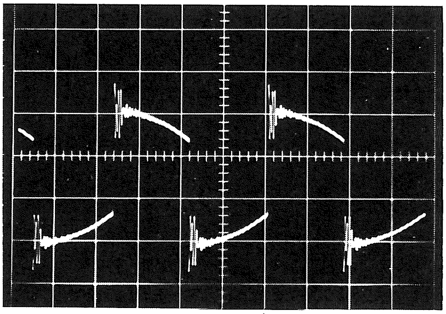

VERTICAL 2 mV/DIV
HORIZONTAL 2 mSEC/DIV
BANDWIDTH DC TO 3 kHz

Fig. 6-41.

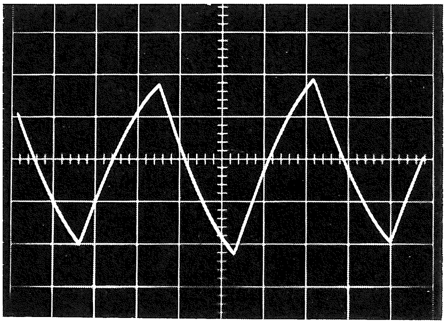

VERTICAL 0.1 V/DIV
HORIZONTAL 2 mSEC/DIV
BANDWIDTH DC TO 1 MHz

Fig. 6-42.

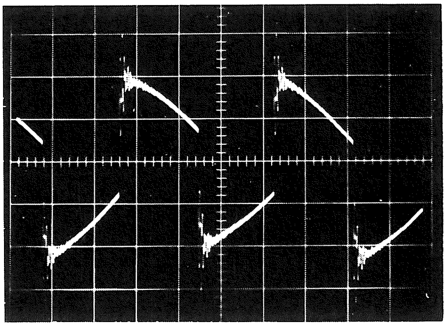

VERTICAL 0.5 mV/DIV
HORIZONTAL 2 mSEC/DIV
BANDWIDTH 10 kHz TO 1 MHz

Fig. 6-43.

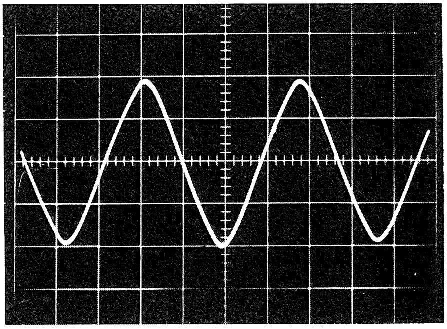

VERTICAL 50 mV/DIV
HORIZONTAL 2 mSEC/DIV
BANDWIDTH OPEN

Fig. 6-44.

The waveform in Fig. 6-44 shows the actual displacement of the shake table and its load being driven by the 60-Hz voltage squarewave. Being the integral of the velocity waveform of Fig. 6-42, it tends to be more sinusoidal because of the attenuation of higher frequency components.

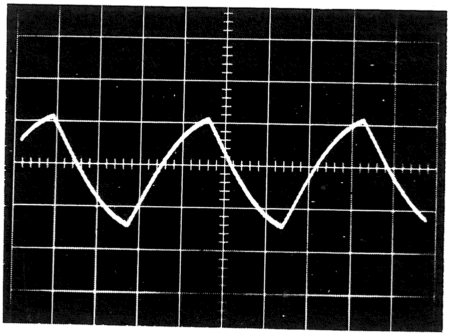

VERTICAL 50 x $10^{-6}$ V/DIV
HORIZONTAL 2 mSEC/DIV
BANDWIDTH UPPER: 1 MHz
LOWER: 10 kHz

Fig. 6-45.

Differentiating the displacement waveform by raising the lower bandwidth limit to 10 kHz (Fig. 6-45) shows that although attenuated by the differentiation process, the waveform is a close replica of the velocity waveform shown in Fig. 6-42.

At the 60 Hz frequency used in this demonstration, integration cannot be performed with the bandwidth controls. At frequencies of 300 Hz and above, however, integration operations can be performed on waveforms in a manner similar to that described above to demonstrate important mathematical relationships between various quantities of motion.

Visual demonstration of fundamental physical laws and relationships has always been regarded as a basic educational tool. The 3A10 transducer measurement system should prove invaluable, therefore, in physical science departments of most modern educational institutions.

# APPENDIX C

## STRAIN GAGE POWER DENSITY GRAPHS

On the following pages are power density graphs for strain gages of three different resistance values. To use these graphs, first determine the power density range for the type of measurement and the material on which the strain gage is to be mounted (see table below). Next, determine the grid area for the strain gage to be used. Enter the graph with these figures to find the maximum safe bridge voltage (not the voltage across the strain gage) for the measurement.

EXAMPLE:

A highly accurate measurement is desired, using a 120-Ω M-M strain gage Type 125BT, whose grid area is 0.0075 $in^2$. The material under measurement is thin stainless steel. Dynamic conditions (frequency) are expected to be encountered. From the table it is seen that under these conditions the power density range is 2 to 10 watts/$in^2$. The intersections of the vertical line representing the grid area and the slanted lines representing these power density levels, when extended to the vertical scale, show the range of safe bridge voltages that can be used under the conditions of the measurement. In this example, the safe bridge voltage range is seen to be about 3 to 6 volts, with 6 volts as a maximum safe level.

HEAT-SINK CONDITIONS

| ACCURACY REQUIREMENTS | | *EXCELLENT*<br>HEAVY ALUMINUM OR COPPER SPECIMENS | *GOOD*<br>THICK STEEL SPECIMENS | *FAIR*<br>THIN STAINLESS-STEEL OR TITANIUM | *POOR*<br>FILLED PLASTICS SUCH AS FIBERGLASS/EPOXY | *VERY POOR*<br>UNFILLED PLASTICS SUCH AS ACRYLIC OR POLYSTYRENE |
|---|---|---|---|---|---|---|
| *STATIC* | HIGH | 2.-5. | 1.-2. | .5-1. | .1-.2 | .01-.02 |
| | MODERATE | 5.-10. | 2.-5. | 1.-2. | .2-.5 | .02-.05 |
| | LOW | 10.-20. | 5.-10. | 2.-5. | .5-1. | .05-.2 |
| *DYNAMIC* | HIGH | 5.-20. | 5.-10. | 2.-10. | .5-1. | .01-.05 |
| | MODERATE | 10.-20. | 10.-20. | 5.-10. | 1.-2. | .02-.1 |
| | LOW | 20.-50. | 20.-50 | 10.-20. | 1.-5. | .2-.5 |

It is of interest to note that most good commercial strain indicators utilize excitation voltages of 3 to 5 volts. The power densities created in gages of various sizes and resistances by these bridge voltages can be directly taken from the charts, and compared with the table above. For very small gages, it is evident that commercial instruments may require voltage reduction for proper results. A simple circuit modification, which may be utilized when the instrument voltage is not adjustable, involves the insertion of 'dead' resistance in the form of high-precision resistors of the Vishay type in series with the active and dummy gages in the external half-bridge. Power density is then reduced by the factor $\frac{R_D + R_G}{R_G}^{2}$, where $R_D$ is the inactive series resistance in ohms, and $R_G$ is the active gage resistance in ohms. Note that the adjacent bridge arm must be increased by the same $R_D$ to maintain bridge balance under these conditions. The sensitivity of the strain indicator will be decreased by this procedure, and the readings must be multiplied by the ration of $\frac{R_D + R_G}{R_G}$ to correct for this desensitization.

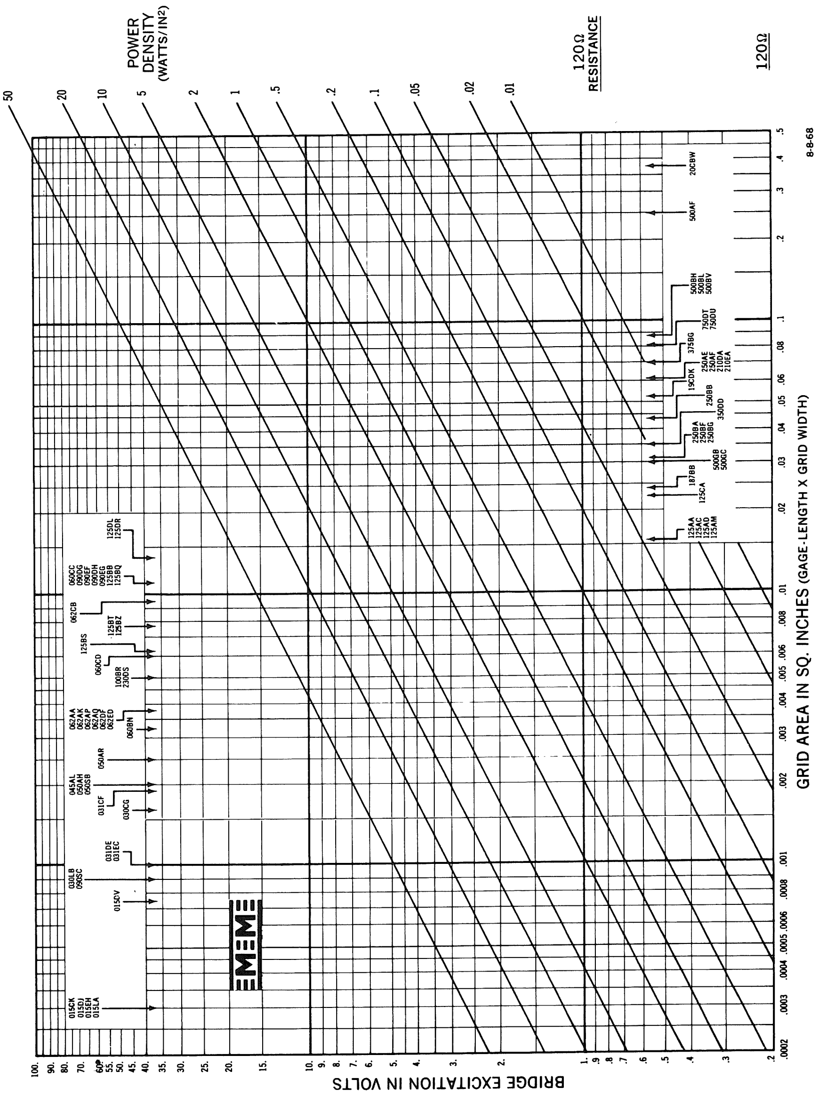
POWER DENSITY (WATTS/IN²)
120Ω RESISTANCE
120Ω
GRID AREA IN SQ. INCHES (GAGE-LENGTH X GRID WIDTH)
BRIDGE EXCITATION IN VOLTS
8-8-68

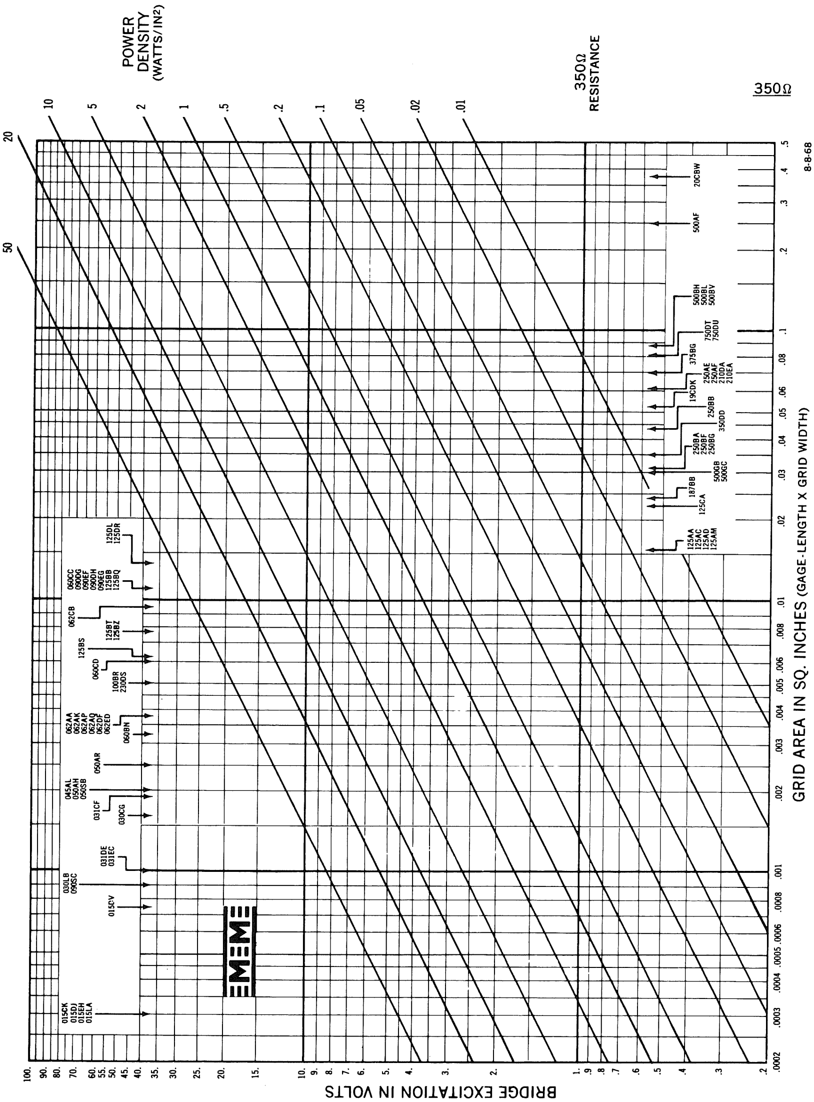
POWER DENSITY (WATTS/IN²)
350Ω RESISTANCE
350Ω
BRIDGE EXCITATION IN VOLTS
GRID AREA IN SQ. INCHES (GAGE-LENGTH X GRID WIDTH)
8-8-68

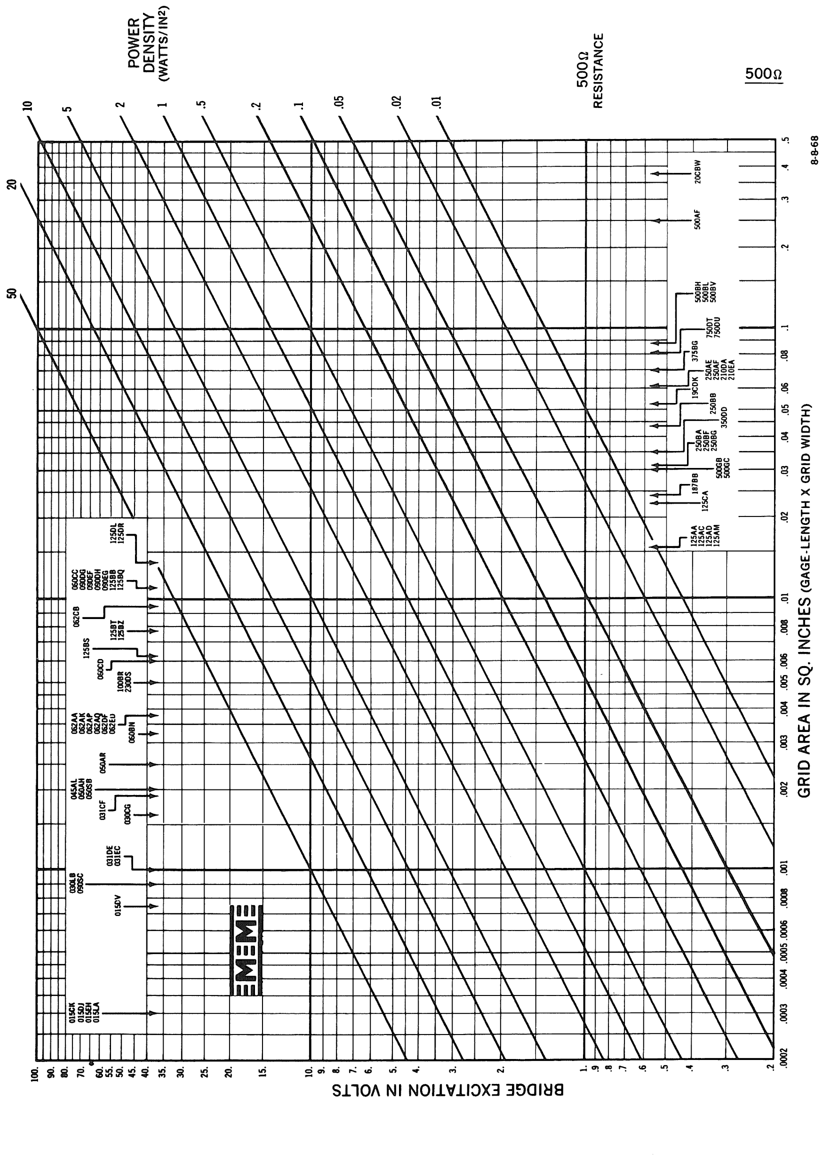
POWER DENSITY (WATTS/IN2)
50
20
10
5
2
1
.5
.2
.1
.05
.02
.01
500Ω RESISTANCE
500Ω
GRID AREA IN SQ. INCHES (GAGE-LENGTH X GRID WIDTH)
BRIDGE EXCITATION IN VOLTS
8-8-68

# APPENDIX D

## VIBRATION NOMOGRAMS

The first vibration nomogram is based on the interrelationship between displacement, velocity, acceleration and frequency as explained in Chapter 3. To use the nomogram, enter with the frequency value and read up to its intersection to the other known value. This intersection point becomes the reference for finding the third unknown.

Example 1: $f$ = 10 Hz, $v$ = 10 in/s

At the intersection of the 10 Hz and 10 inches/second lines, the value of acceleration (negative slope lines) is about 1.75 $g$ while that of displacement (positive slope lines) is about 0.175 inches.

Example 2: $f$ = 10 Hz, displacement = 1 inch

At the intersection of the 10Hz and 1 inch lines, velocity is 62.8 ($2\pi$ X 10) inches/second and acceleration is exactly 10 $g$.

The second vibration nomogram is scaled only in frequency and displacement. The heavy lines indicate the relative severity of machinery vibration. Note that vibration becomes more severe as displacement amplitude and frequency of vibration increase, since either affect tends to increase the *peak acceleration* of that vibration.

VIBRATION NOMOGRAM

RELATION OF DISPLACEMENT, VELOCITY, AND ACCELERATION IN PURE SINUSOIDAL VIBRATION
ALL QUANTITIES MUST BE READ IN THE SAME RELATIVE AMPLITUDE
(i.e., SINGLE AMPLITUDE OR DOUBLE AMPLITUDE)

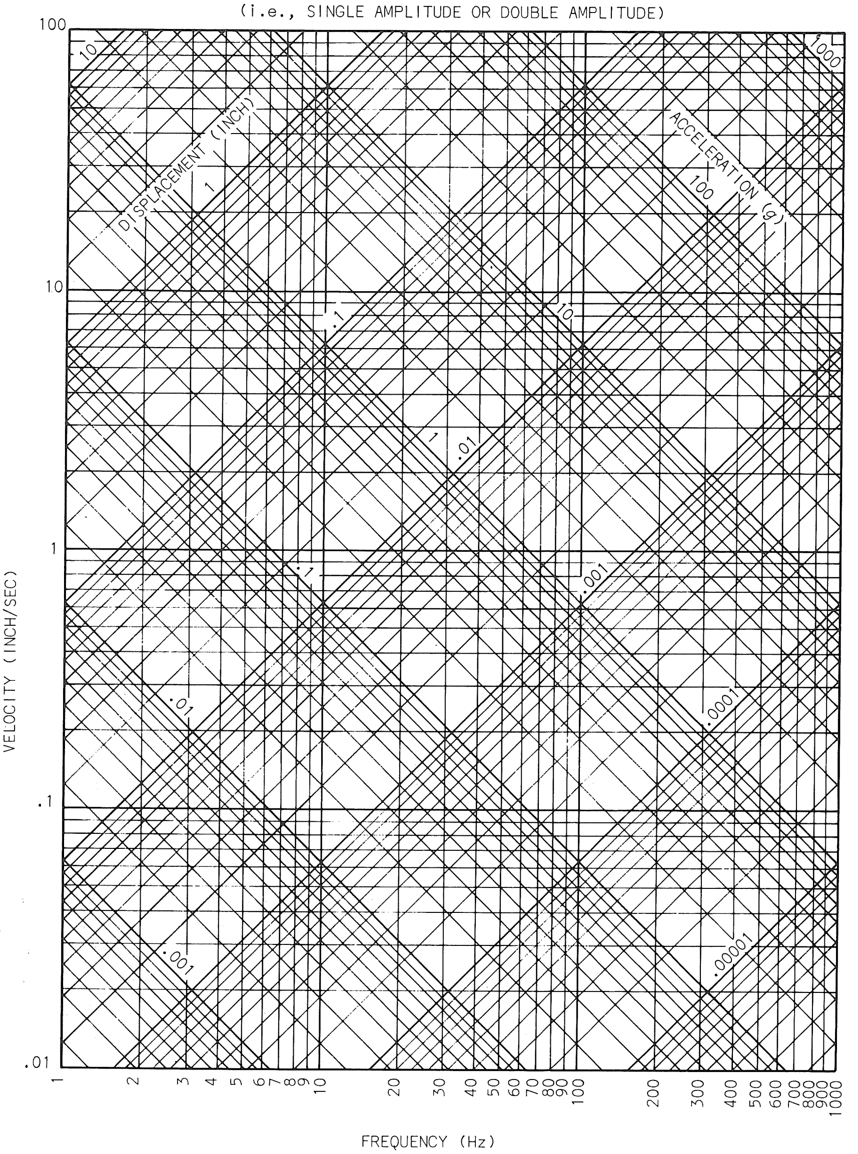

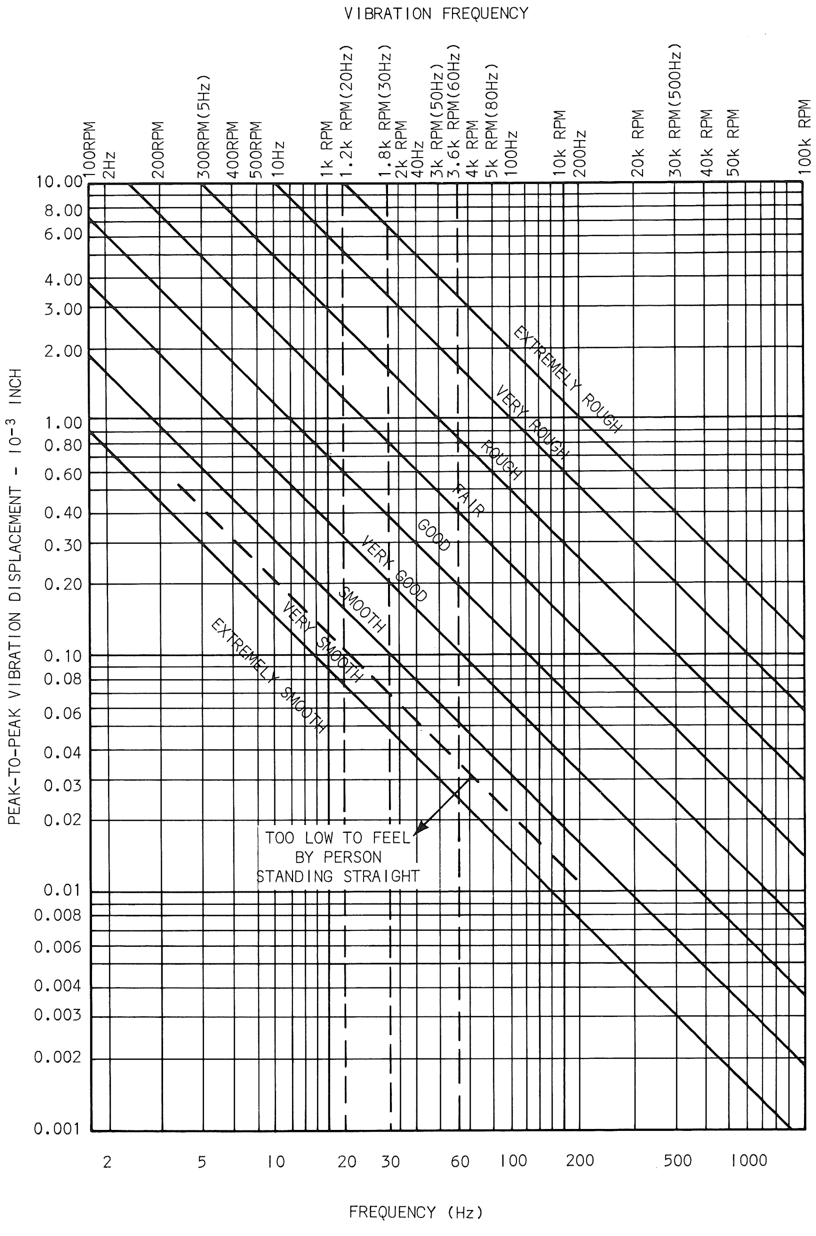


SEVERITY OF MACHINERY VIBRATION

# NOTES

# NOTES